ABSTRACT

Biochemical Studies of Cathepsin B and Cruzain Inhibitors Sharing a Thiosemicarbazone
Moiety

Victoria Soeung

Director: Mary Lynn Trawick, Ph. D

Over-expression of cysteine proteases has been implicated in a number of diseases, making them attractive targets for drug design. The cysteine protease, cathepsin B has been implicated in the degradation of the extracellular matrix and thereby facilitates tumor cell metastasis and invasiveness, suggesting that inhibition of cathepsin B may be an important target for anti-cancer treatment. Natural and synthetic inhibitors of cathepsin B have demonstrated selective enzyme inhibition, but many of these compounds exhibit peptidic characteristics, reducing their bioavailability. A separate cysteine protease, cruzain, is essential for the survival of *Trypanasoma cruzi*, the causative agent of Chagas' disease and is involved in parasitic nutrition, replication, and evasion of the host immune system. In these studies, a library of small non-peptidic compounds that share a thiosemicarbazone moiety were analyzed against cathepsin B and cruzain. A number of thiosemicarbazone derivatives were found that exhibited IC_{50} values (the concentration of compound that resulted in fifty percent enzyme inhibition) in the lower micro-molar and nano-molar range against cathepsin B and cruzain respectively. Fluorometric microplate assays were used to determine IC_{50} values as a measure of effectiveness of the compounds. Advanced kinetic studies were conducted on cathepsin B in order to determine the mechanism of inhibition. Analysis of the structure activity relationships (SAR) of these compounds show promising results for drug design. These studies represent collaborative research between the Trawick (biochemistry) and Pinney (organic synthesis) Laboratories.

APPROVED BY DIRECTOR OF HONORS THESIS:

_____

Dr. Mary Lynn Trawick

Department of Chemistry and Biochemistry

APRROVED BY THE HONORS PROGRAM:

_____

Dr. Andrew Wisely, Director

DATE: _____

BIOCHEMICAL STUDIES OF CATHEPSIN B AND CRUZAIN INHIBITORS

SHARING A THIOSEMICARBAZONE MOIETY

A Thesis Submitted to the Faculty of

Baylor University

In Partial Fulfillment of the Requirements of the

Honors Program

By

Victoria Soeung

Waco, Texas

May 2012

TABLE OF CONTENTS

LIST OF FIGURES

LIST OF TABLES

LIST OF EQUATIONS

LIST OF ABBREVIATIONS

°C	Degrees Celsius
AD	Alzheimer's Disease
AMC	7-amino-4-methylcoumarin
APP	Amyloid β-precursor protein
DMSO	Dimethyl Sulfoxide
DTT	Dithiothreitol
EDTA	Ethylenediaminetetraacetic acid
IBC	Inflammatory Breast Cancer
IC_{50}	Median Inhibitory Concentration
MBC	Molecular Bioscience Center
NADPH	nicotinamide adenine dinucleotide phosphate-oxidase
T. cruzi	*Trypanasoma cruzi*
TSC	Thiosemicarbazone
Z-RR-AMC	Benzyloxycarbonyl-L-arginyl-L-arginyl-7-amido-4-methylcoumarin

ACKNOWLEDGEMENTS

this study. Lastly, I would like to thank Baylor University for their financial support that

made this research possible.

CHAPTER ONE

Statement of the Problem and Significance of the Study of Cathepsin B

Introduction to Cancer

The term cancer encompasses a range of diseases that involve cells that divide uncontrollably and that eventually invade other tissues.[1] The etiology of cancer is multifactorial involving environmental, genetic, medical, and lifestyle factors.[2] Cancer can be subdivided into broad categories based on the origin of the cancerous cells. Carcinoma cancer begins in the skin or tissues that line internal organs. Sarcoma cancer begins in the bone, cartilage, fat, muscle, blood vessels, or other connective or supportive tissue. Leukemia cancer begins in blood-forming tissues such as bone marrow. Lymphoma and myeloma cancer begins in the cells of the immune system. Central nervous system cancer begins in tissue of the brain or spinal cord. Stages are typically indicated by Roman numerals, I through IV, with the higher numbers indicating more advanced cancer.[3] In the year 2007, the estimated prevalence of cancer in the United States alone is approximately twelve million people. [4]

Description of Cancer

Normal cells in the body should divide in a controllable manner and be replaced when they become useless via mechanisms such as apoptosis. Apoptosis is a mechanism of natural cell death that removes unwanted cells, allowing the body to function properly. However, mutations may occur that disrupt the natural cell life cycle, causing uncontrolled division or growth of cells (Figure 1). Eventually, the uncontrolled growth

of cells causes cells to pile up on one another, creating an abnormal mass of tissues called a tumor which may lead to cancer. However, not all tumors are cancerous because they do not affect other tissues. These tumors are benign because they do not metastasize and usually do not reform after surgical removal. Malignant tumors, however, are cancerous and infect other tissues in the body by spreading cancerous cells via entrance into the blood stream and lymph system.
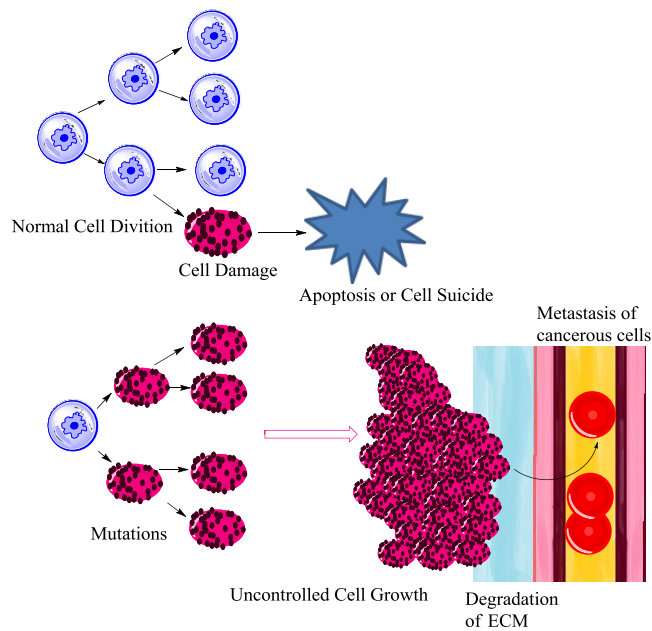
Figure 1. Normal cell division and cancerous cell division (Figure adapted from National Cancer Insitute)

Signs and symptoms of cancer will vary according to the type of cancer. However, cancer is generally associated with fatigue, formation of a lump or thickening that can be felt under the skin, weight change whether unintended loss or gain, skin changes such as yellowing, darkening or redness of skin, sores that will not heal, or changes to existing moles, changes in bowel or bladder habits, persistent cough, difficulty swallowing, hoarseness, persistent indigestion, and/or persistent and unexplainable muscle or joint pain. [5]

Current Treatment for Cancer

Current treatment for cancer includes chemotherapy, radiation therapy, and surgical procedures such as cryosurgery.[7] However, these current methods have many risks and side effects. For instance, chemotherapy may result in anemia, appetite changes, bleeding problems, constipation, diarrhea, fatigue, alopecia (hair loss), memory loss, nausea and vomiting, neuropathy (numbness or tingling in parts of body), and lower blood cell count which may increase the chances of infection.[8] Although survival rates are improving due to improved cancer screening and treatment, cancer remains the second-leading cause of death in the United States.[9]

Introduction to Proteases

Proteases are enzymes that catalyze the breakdown of proteins and polypeptides by hydrolysis of peptide bonds. Protease may also serve as subtle means of protein activation and regulation.[10] There are two basic types of proteases, endopeptidases and exopeptidases. Endopeptidases cleave protein substrate at a peptide bond within the amino acid sequence. On the other hand, exopeptidases cleave protein substrate at the end of the protein, either the C-terminal or N-terminal. Proteases are also classified by their differing mechanism of action. For instance, if a protease works by covalent catalysis, the protease may be classified as a serine, cysteine, or threonine protease. The protease of interest in this study is cathepsin B, a cysteine protease.

Cysteine Proteases

Lysosomal cysteine proteases are generally known as cathepsins and are generally found in the lysosome of a cell. Cathepsin is derived from the Greek work for digest and

describes the basic function of the proteases. There are currently eleven known human cysteine cathepsin proteases, cathepsin B, C, F, H, K, L, O, S, L/V, W, and X/Z.[11] These proteases are known as papain like because of their conserved active site that resembles the active site of papain, a protease of papaya. The active site of the cathepsin proteases all share a conserved cysteine and histidine residue.[2] This study focuses specifically on the cysteine protease, cathepsin B, and its pathological implications and potential pharmaceutical drugs that function via the inhibition of cathepsin B.

Processing of Procathepsin B

Cathepsin B is the most abundant lysosomal cysteine protease in mammalian tissue.[12] Cathepsin B like other cathepsins is synthesized as an inactive precursor known as a proenzyme. Procathepsin B is approximately 38 kDa. Procathepsin B is similar in structure to mature cathepsin B. However, there is a difference near the occluding loop domain of cathepsin B (Ile-105 through Pro-126). In mature cathepsin B, the occluding loop blocks the active site cleft from behind. However, in the procathepsin form, the occluding loop is lifted away from the enzyme surface and interacts with the propeptide (Figure 2).[16]

Cathepsin B is initially synthesized as a preproenzyme in the rough endoplasmic reticulum. Intracellular transport of procathepsin B relies on either a mannose-6-phosphate receptor system or a mannose 6-phosphate independent pathway.[13] After removal of signal peptide during the passage into the endoplasmic reticulum, glycosylated proenzymes undergo proteolytic processing into the active form of cathepsin B.[14] The propeptide of cathepsin B is a predominantly α-helical domain which is positioned like a hook at the top of cathepsin B's catalytic site. The propeptide extends

across the entire active site cleft towards the N-terminus in an inverted conformation to the binding conformation of substrate, preventing substrate hydrolysis and making the enzyme inactive (Figure 3).[15]

<div align="center">(a)   (b)</div>
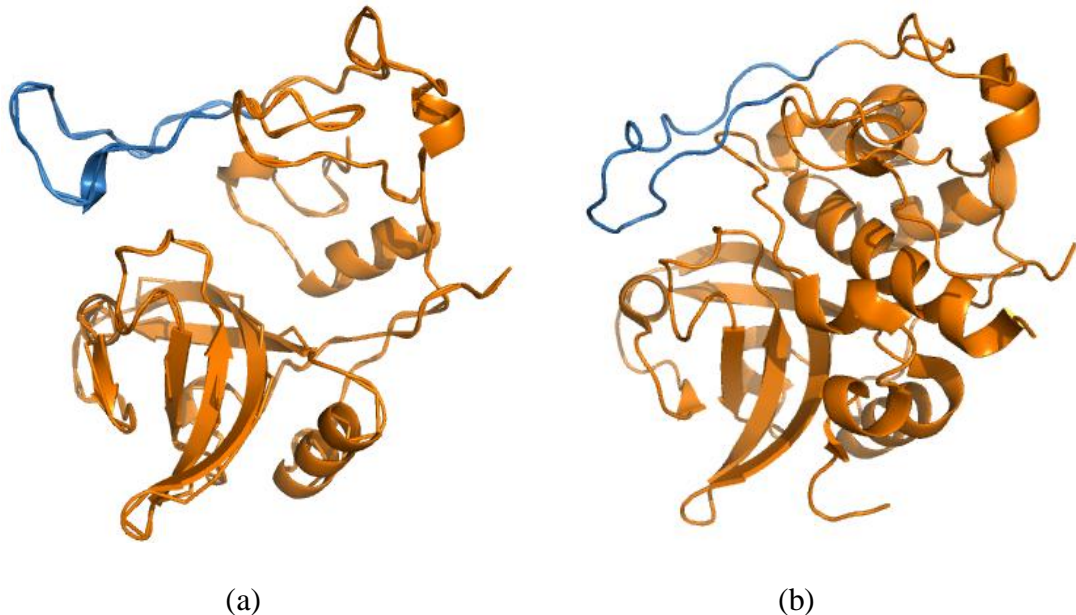
Figure 2. (a) Crystal structure of procathepsin B. Occluding loop depicted in blue.Propeptide is not depicted. (adapted form, PDB 2PBH Turk et al.)[16] (b) Crystal structure of mature cathepsin B. Occluding loop depicted in blue.[16] (adapted from PDB 2IPP, Huber *et al.*)

Cathepsin B is activated by proteolytic removal of the N-terminal propeptide. Activation *in vitro* can be caused by[17]:

1. Activation by other proteases such as pepsin or cathepsin D

2. Autocatalytic activation at acidic pH.

Autocatalytic activity of cysteine cathepsins have been shown to be accelerated by the presence of glycosaminoglycans.[14] The optimum pH for autocatalytic activity *in vitro* is approximately 4.5.[15]

Figure 3. Crystal structure of procathepsin B. Occluding loop is depicted in green and propeptide is depicted in teal. (Adapted from PDB 2PBH, Turk et al)[18]

Structure of Mature Cathepsin B

Initially human procathepsin B weighs approximately 38 kDa.[20] However after processing and loss of the propeptide, mature cathepsin B (EC. 3.4.22.1) weighs approximately 24 – 35 kDa depending on the amount of glycosylation present.[13] Cathepsin B is larger than papain. Mature cathepsin B can exist as a single chain form, a double chain form, or both (Figure 4).[21] Purified cathepsins are generally composed of disulfide connected light and heavy chains.[16] Cathepsin B has six disulfide bridges. It also consists of a light chain running from Lys 1 to Arg 49 and a heavy chain running from Val 50 to Thr 253.[22] Human Cathepsin B has fourteen cysteine residues. Cys 29 represents the active site cysteine residue. Cys 240 remains unpaired and is unique to cathepsin B. Twelve of the other cysteine residues are presumed to be involved in disulfide bridges.[23]

Cathepsin B activity is optimal at acidic pH and becomes irreversibly deactivated at basic pH. [14] The instability of cathepsin B at neutral or alkaline pH may be a defense mechanism to keep unwanted cysteine proteases out of the extracellular matrix. Wild type human cathepsin B cannot refold after exposure to neutral or alkaline pH. However, removal of the Cys 29 residue and replacement with an alanine residue allowed a human cathepsin B mutant to refold after exposure to neutral or alkaline pH when returned to acidic pH, confirming that the Cys 29 residue is involved in the refolding barrier for cathepsin B.[24]

A proposed mechanism of action for the pH dependant inactivation of cathepsin B is summarized below:

1. Deprotonation of His 199 is catalyzed by an hydroxide ion

2. Thiolate from Cys 29 – imidazolium from His 199 pair is broken, exposing some charged residues

3. Enzyme is critically unstable and unfolds, changing the α-helical region where the Cys 29 is located[25]

Inactivation of cathepsin B is followed by a dramatic decrease in α-helical content whereas β-sheet content apparently increases. The change in α-helical and β-sheet content confirms that inactivation of cathepsin B is induced by a conformational change in the enzyme.[21]

Like papain, Cathepsin B is bilobal, consisting of two domains, a left domain and a right domain (Figure 5). The left domain (L-domain) is dominated by three α-helices. The three α-helices are arranged perpendicularly. The left domain is formed by the N-terminal half of the polypeptide chain and by the last four C-terminal residues. The L-

domain of cathepsin B is largely hydrophobic consisting of eighteen hydrophobic residues. On the left domain, cathepsin B crosses over itself at Cys 108 and Cys 119 via a disulfide bridge which creates a covalently closed structure called the occluding loop. The occluding loop is unique to cathepsin B.[21]

Cys 29

```
          10              20              30              40              50
MWQLWASLCC    LLVLANARSR    PSFHPLSDEL    VNYVNKRNTT    WQAGHNFYNV

          60              70              80              90              100
DMSYLKRLCG    TFLGGPKPPQ    RVMFTEDLKL    PASFDAREQW    PQCPTIKEIR

          110             120             130             140             150
DQGSCGSCWA    FGAVEAISDR    ICIHTNAHVS    VEVSAEDLLT    CCGSMCGDGC

          160             170             180             190             200
NGGYPAEAWN    FWTRKGLVSG    GLYESHVGCR    PYSIPPCEHH    VNGSRPPCTG

          210             220             230             240             250
EGDTPKCSKI    CEPGYSPTYK    QDKHYGYNSY    SVSNSEKDIM    AEIYKNGPVE

          260             270             280             290             300
GAFSVYSDFL    LYKSGVYQHV    TGEMMGGHAI    RILGWGVENG    TPYWLVANSW

          310             320             330
NTDWGDNGFF    KILRGQDHCG    IESEVVAGIP    RTDQYWEKI
```

His 199

Asn 281

Signal Peptide (Residues 1-17)
Propeptide (Residues 18-79 and 334-339)
Light Chain (Residues 80-126)
Heavy Chain (Residues 129-333)
•••••• Disulfide Bonds
Mature Cathepsin B (Residues 80-333)

Figure 4. Uniprot.org amino acid sequence of human cathepsin B [26]

8
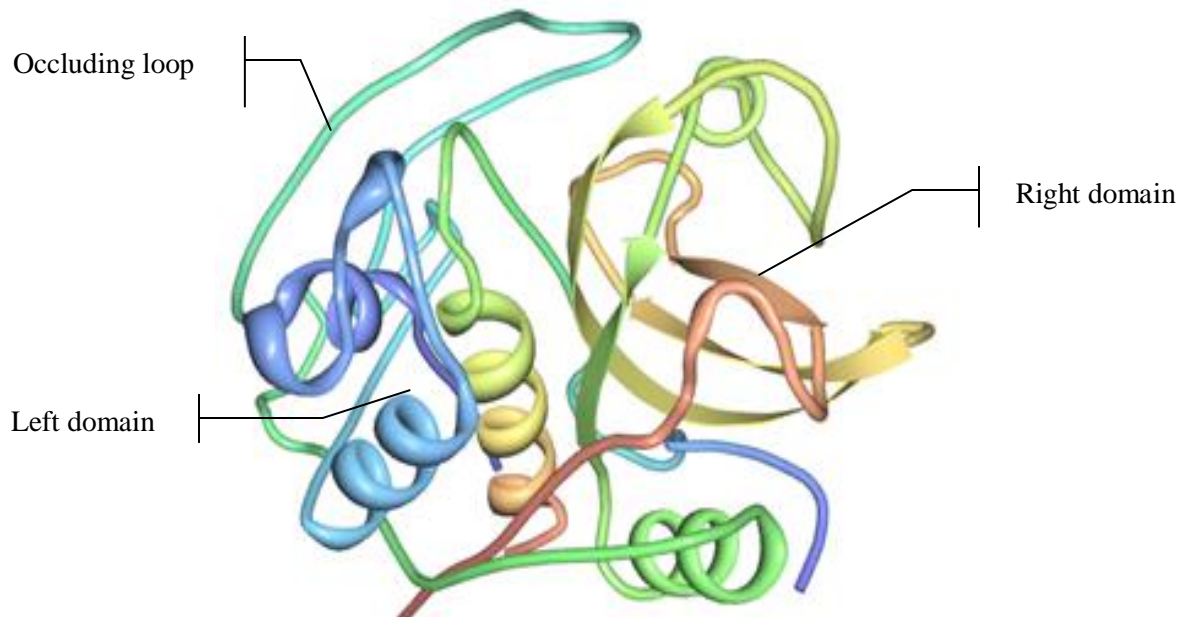
Figure 5. Crystal structure of cathepsin B. Occluding loop is depicted in cyan and located on the left. Three perpendicular α-helices can be seen on the left domain under the occluding loop. The β-barrel motif enclosed by two α-helices can be seen on the right domain (Adapted from PDB IHUC, Musil et al)[27]

The Right Domain

The right domain (R-domain) consists of six extended strands that are arranged in β-sheets that are anti-parallel to each other. These β-sheets are highly twisted and bent into a β-barrel motif. The β-barrel is closed at both ends with α-helical segments. The right domain encloses a highly hydrophobic core. It possesses many aromatic residues and almost all the charged residues are located on the surface. Only three charged residues extend into the interface of the right domain β-barrel, Glu 171, Arg 202, and Asp 224. The right domain is composed of the carboxy-terminal half of the polypeptide chain.[21]

9

The Inter-domainal Space/ Active Site

Both the amino and carboxy-terminal ends strap and clamp the left and right domains together. Both domains are in contact and enclose a water filled channel. Water molecules are located in the active site to keep the domains from collapsing onto each other. When a substrate binds to the active site, it must move the water out of the binding cleft. The domains are clamped together but begin to diverge, creating a v-shaped active site cleft (Figure 6). The occluding loop, located on the left domain, blocks the active site from the rear at neutral pH. [21] In the environment of the active site, thiol and imidazole side chains of Cys 29 and His 199 respectively form an ion pair over the pH ranges of 4.0 – 8.5.[28] The Cys 29 is located on the left domain, and the His 199 is located on the right domain. The catalytic triad of cathepsin B is composed of Cys 29, His 199, and Asn 281.[19] Substrate cleavage involves nucleophilic attack by the thiolate ion on Cys 29 residue and proton donation from the imidazole group of His 199 residue.[26]

Occluding Loop

The occluding loop is an eighteen residue long insertion located on the left domain and unique to cathepsin B (Figure 7).[29] It blocks the active site cleft from the rear, keeping substrate from binding within the active site pocket at acidic pH and making cathepsin B behave as an exopeptidase.[30] Thanks to the occluding loop, cathepsin B has a dual role and may behave as either an endopeptidase or an exopeptidase, depending on pH. At acidic pH such as within the lysosome, exopeptidase activity dominates. At neutral pH such as when cathepsin B is in the extracellular matrix,

endopeptidase activity dominates. [25] Cathepsin B's ability to perform endopeptidase activity at neutral pH suggests that cathepsin B may be one of the proteolytic enzymes that degrade extracellular membrane and basement membrane during tumor invasion and metastasis.
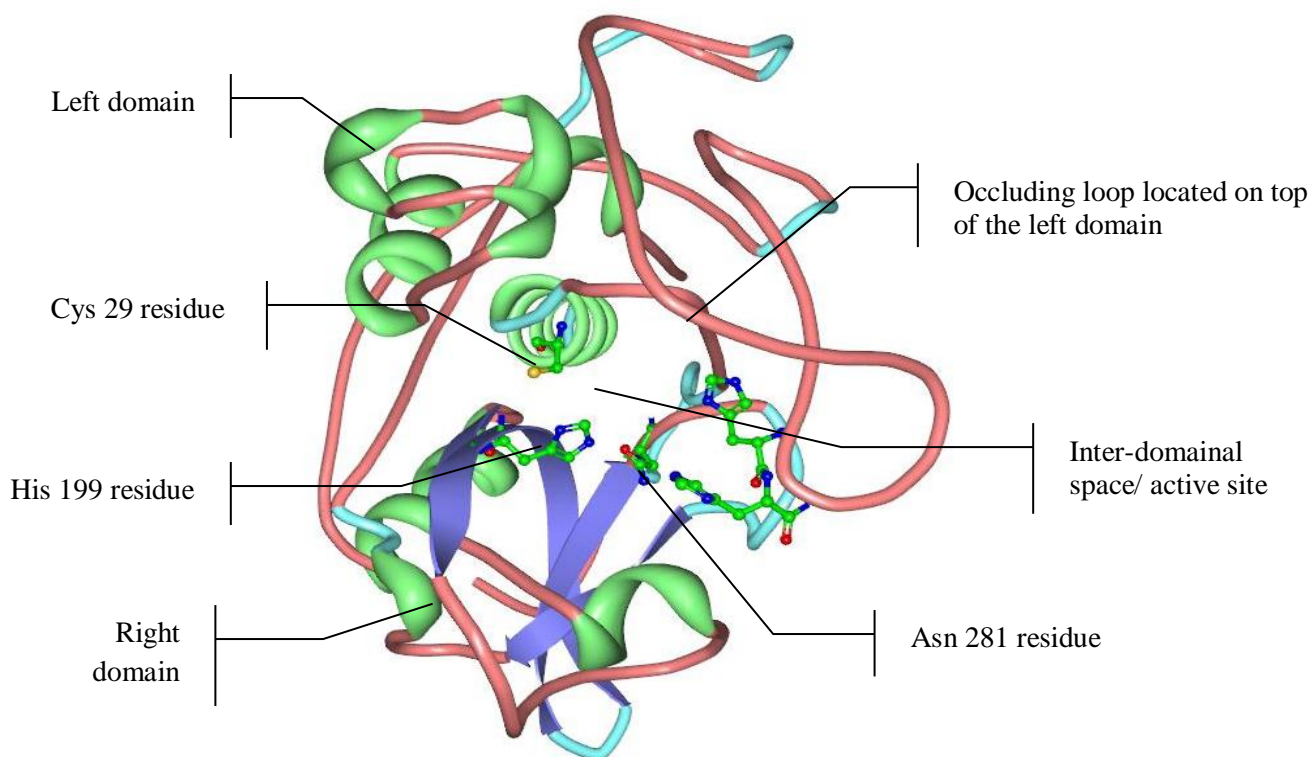
Figure 6. Upward view of cathepsin B with left domain located on top and right domain located on the bottom. (Adapted from PDB 1HUC, Adapted from Musil et al)[25]

The exopeptidase activity or peptidyldipeptidase activity of cathepsin B at the carboxyl-terminal most likely depends on two residues, His 110 and His 111, located on the occluding loop. At acidic pH, two salt bridges form between Asp 22 – His 110 and Arg 116 – Asp 224, holding the usually flexible occluding loop in a closed position over the active site of the mature enzyme (Figure 5). At neutral or alkaline pH, the salt bridges break and the occluding loop no longer is clamped over the active site, allowing endopeptidase activity.[31]
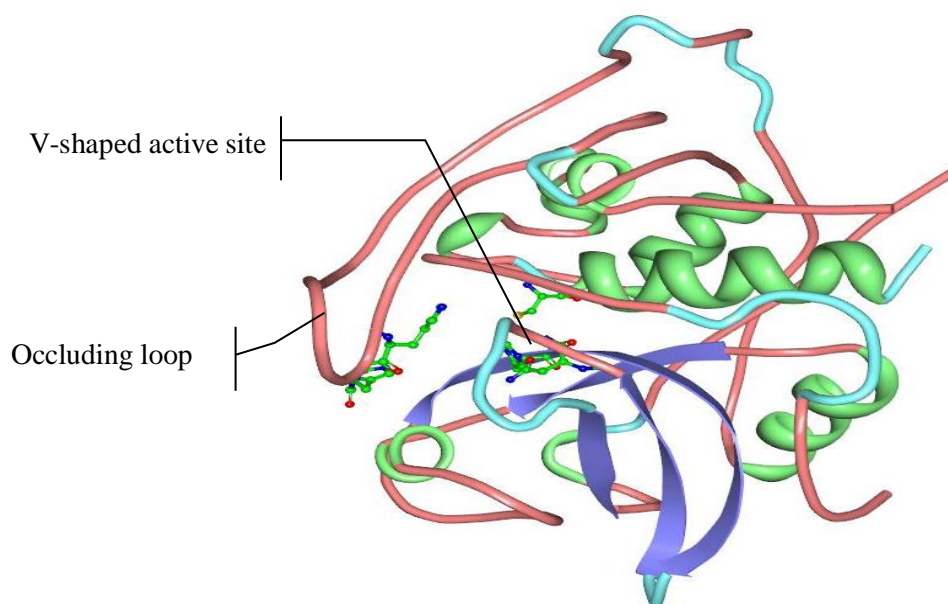
Figure 7.Sideways view of cathepsin B. Occluding loop blocks v-shaped active site at neutral pH. (Adapted from PDB 1HUC, Musil et al)[25]

The His 110 residue remains unpaired whereas the His 111 residue participates in a salt bridge with Asp 22. Site directed mutagenesis of His 111 demonstrates that His 111 makes a tenfold contribution to the exopeptidase activity of cathepsin B. However, it is not critical for exopeptidase activity. [29] On the other hand, His 110 is essential for exopeptidase activity of cathepsin B. The interaction between His 110 and Asp 22 stabilizes the interaction between the imadazolium ion and substrate C-terminal carboxylate by a maximum of 13.9kJ/mol (Figure 8).[29]

Mutational deletion of the entire occluding loop eliminates exopeptidase activity while keeping endopeptidase activity. Removal of His 111 decrease exopeptidase activity by tenfold. Removal of Asp 22 – His 110 and Arg 116 – Asp 224 ion pairs leads to a drastic increase in endopeptidase activity.[27] In summary, the role of the occluding loop is to allow exopeptidase activity of cathepsin B. The key role of the Asp 22 – His 110 salt

bridge is to position the occluding loop for exopeptidase activity. The key role of His 111 is to provide an anchor for C-terminal carboxylate of the substrate, contributing to the substrate C-terminal binding to the active site.
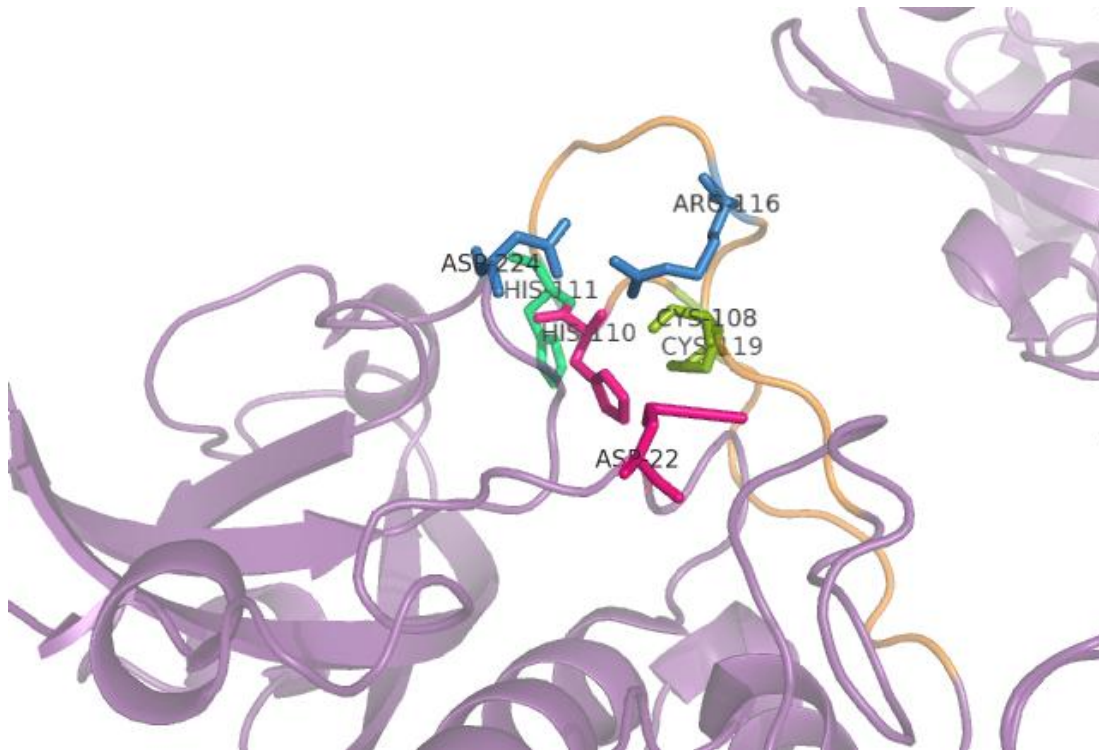
Figure 8.Salt bridges form between Arg 116 and Asp 224 (depicted in blue) and His 110 and Asp 22 (depicted in pink). His 111 (cyan) remains unpaired and Cys 108 and Cys 119 form a disulfide bond (depicted in green). (Adapted from PDB 1HUC, Musil et al)[25]

The occluding loop is also thought to contribute to cathepsin B's lower affinity towards potent inhibitors of other papain like enzymes. For instance, deletion of the occluding loop led to a fortyfold higher affinity between cathepsin B and cystatin C.[32] Binding of the cathepsin B propeptide to cathepsin B was increased fiftyfold with removal of the occluding loop.[28] Shortening of the occluding loop led to an increase in

13

the binding affinity of the free procathepsin B to mature cathepsin B. Likewise inhibitors tested on cathepsin B were one-hundredfold less active than the rates for cathepsin L.[33]

Subsites

The S_1, S_2, S_3, S_4, S_1', S_2', and S_3' binding pockets or subsites in cathepsin B have been defined. The region of the inhibitor or substrate that bind to each respective subsite is named P_1, P_2, P_3, P_4, P_1', P_2', and P_3'. The primed subsites of cathepsin B bind to the C-terminus and the unprimed subsites bind to the N-terminus of the substrate. Since the shape and size of the binding pockets of papain and cathepsin B are similar, the differences in substrate binding specificity is most likely due to the spatial orientation and functionality of the residues which construct the subsites.[34]

Enzymes with exopeptidase activity have features such as the occluding loop in cathepsin B that reduce the number of binding sites.[13] Based on the structure of bovine cathepsin B complexed with a epoxysuccinyl derivative both *in vitro* and *in vivo,* there are three well defined subsites on cathepsin B, S_2, S_1, S_1', which involve both the main and side chain interactions between substrate and enzyme residues.

The Unprimed Subsites

The unprimed subsites are located towards the C-terminal side of the scissile bond. The S_1 subsite includes Cys 29. It is located on the left domain[27] at the active center and corresponds to the oxyanion hole.[35] The hydrophobic S_2 pocket is formed by Pro 76, Ala 173, Gly 198, and Ala 200.[33] It is a shallow hydrophobic depression.[29] The S_2 subsite is speculated to be the primary determinant of substrate specificity. The S_2 pocket prefers a hydrophobic residue as P_2. The S_2 pocket is sufficiently large to accommodate a large

variety of P_2 substituents. The S_2 and S_3 subsites are located on opposite sides of a funnel shaped entrance into the active site cleft.[36] The S_3 subsite is not well defined but past experiments indicate that cathepsin B may prefer hydrophobic residues such as Leu, Tyr, Phe, and Trp at the S_3 subsite.[29] It is uncertain as to whether the S_4 subsite participates in substrate binding. In general cathepsin B accepts hydrophobic residues much more readily than hydrophilic residues. [34]

The Primed Subsites

The primed subsites are located towards the N-terminal of the scissile bond. The $S_1^{'}$ subsite is a hydrophobic pocket, consisting of Val 176, Leu 181, Met 196, His 199, and Trp 221 residues. Since the $S_1^{'}$ subsite is hydrophobic, a hydrophobic substituent at the P_1' site would be most likely be most preferable.[33] The occluding loop is located towards the primed region of the active site and greatly affects the specificity of the S_2' subsite.[35] The S_2' subsite prefers large aromatic residues. For instance, there is a twentyfold difference between substrates containing Trp and Glu residues at the P_2' area.[29] Cathepsin B does not show any clear preference between the different amino acids in the $S_3^{'}$, suggesting that the P_3' site on the substrate or inhibitor does not interact with the cathepsin B enzyme.[34]

Diseases Associated with Cathepsin B

An imbalance in cathepsin B activity regulation has been implicated with a wide range of human diseases such as cancer, rheumatoid arthritis, osteoporosis, and neurological disorders such as Alzheimer's disease.[37] *In vitro* and *in vivo* studies on both

a mouse model and on human cells have supported the pathological functions of cathepsin B.

For instance, high levels of active cathepsin B along with cathepsins H, K, L and S have been detected in inflammatory bronchoalveolar lavage fluid in acute and chronic inflammatory lung disease.[38] Cathepsin B, L, K, and S have also been found in joint cartilage and synovial cells of patients with rheumatoid arthritis and osteoarthritis.[37] It is believed that cathepsin B contributes to cartilage destruction and immune response to people suffering from rheumatoid arthritis. In certain mouse models selective inhibition of catehpsins have had protective effects.[37]

It has also been found that plasma cathepsin B levels are higher in patients suffering from Alzheimer's disease, which is characterized by severe memory loss and neuro-degeneration caused mainly by amyloid-β aggregation into amyloid plaques, than in healthy controls, suggesting that cathepsin B may be involved in amyloid-β processing.[39] Further studies using Morris water maze water test and AD mouse models that express the wild-type β-secretase site of human APP expressed in most humans suffering from Alzheimer's disease showed that selective inhibitors of cathepsin B such as CA074 led to improved memory and reduced amyloid-β peptidase build-up.[40]

Cathepsin B along with cathepsin F,H, K, L, V,S, and X/Z have been implicated with cancer and metastasis. Many cathepsins are overexpressed in carcinomas and are frequently associated with poor prognosis for patients. The implications, pathway, and potential mechanisms involving cathepsin B and cancer are one of the main focuses of this study and are discussed in further detail.

Tumor Progression, Invasion, and Metastasis

Tumorous cells attach to and degrade the basement membrane and extracellular matrix, allowing the tumor to metastasize to distant locations. Various proteolytic enzymes are implicated with tumor progression. One of these enzymes is cathepsin B.[41] Changes in cathepsin B localization and expression have been observed in several human tumor tissues.[42] Increases of cathepsin B expression has been viewed at both the gene level and the protein level. Cathepsin B at the gene level is altered with the use of gene amplification, elevated transcription, use of alternative promoter and alternative splicing.[43] Up regulation of cathepsin B at the gene level leads to subsequent up regulation at the protein level, leading to change in localization and increased secretion and activity of the enzyme.[42]

Cathepsin B expression is greater in tumor cells that are in the stages of invading bowel walls than in tumor cells in later stages, suggesting that cathepsin B may be involved in tumor invasion and degradation of extracellular matrix. [40] Cathepsin B expression is also higher at the invvasive edges or epithelial cells on the outer edges of the premalignant lesions. Likewise macrophages in tumor microenvironment also have increased levels of cathepsin B.[44]

It has been suggested that cathepsin B is secreted in the inactive form and active form. Procathepsin B may be over secreted due to the defects to the normal trafficking pathways for procathepsin B. For instance, pancreatic islets of transgenic mice that lack the 46 kDa mannose-6-phosphate receptor (MPR) pathway display a fourfold increase in expression of procathepsin B in mature secretory vessels that are destined for secretion.[45] It has been suggested that active cathepsin B may be secreted from tumor cells with the

aid of lysosomal exocytosis. In fact, calcium dependent lysosomal exocytosis has been observed in normal cells.[44] Hypoxia in the tumor microenvironment caused by uncontrolled growth of cells results in a more acidic pH which is ideal for cysteine cathespin activity.[46]

The mechanism of cathepsin B degradation of extracellular matrix *in vivo* has yet to be elucidated. However, findings from *in vitro* analysis are helping shed light to how cathepsin B may contribute to extracellular degradation and tumor invasiveness and metastasis. Cathepsin B secreted from the cell or at the cell surface may lead to extracellular degradation. Likewise it can be possible that extracellular matrix is taken into the cell by endocytosis and degraded by intracellular catehpsin B.

In vitro experiments have shown that cathepsin B degrades type IV collagen and enhances invasion of cancerous inflammatory breast cancer (IBC) cells through the use of caveolae at the cell surface.[47] Cathepsin B alsong with the serine protease urokinase plasminogen (uPA), and urokinase plasminogen receptor (uPAR) have all been identified to be localized in caveolae, a subset of lipid rafts, of tumorous cells.[46] Down regulation of the structural protein for cavaeolae formation, caveolin-1, has resulted in a decrease in degradation of collagen type IV and metastatic invasion in colon cancer cells *in vitro*. [48] Cathepsin B has also been shown to activate pro-uPA to active uPA, initiating the plasminogen cascade *in vitro* (Figure 9).[47]

Lysosome or endoplasmic vesicle

Cat D or Cat G

Pro-Cat B → Cat B

Fuses with cell membrane

Enlarged View of
Caveolae

Plasminogen

uPA

Pro-uPA

Plasmin

Cat B

pro-MMP

MMPs

Degrades many
components
of ECM including
collagen I and IV,
gelatins, and
proteoglycan

Degrades several
components of
ECM including
fibrin, fibronectin,
proteoglycan, and
laminin
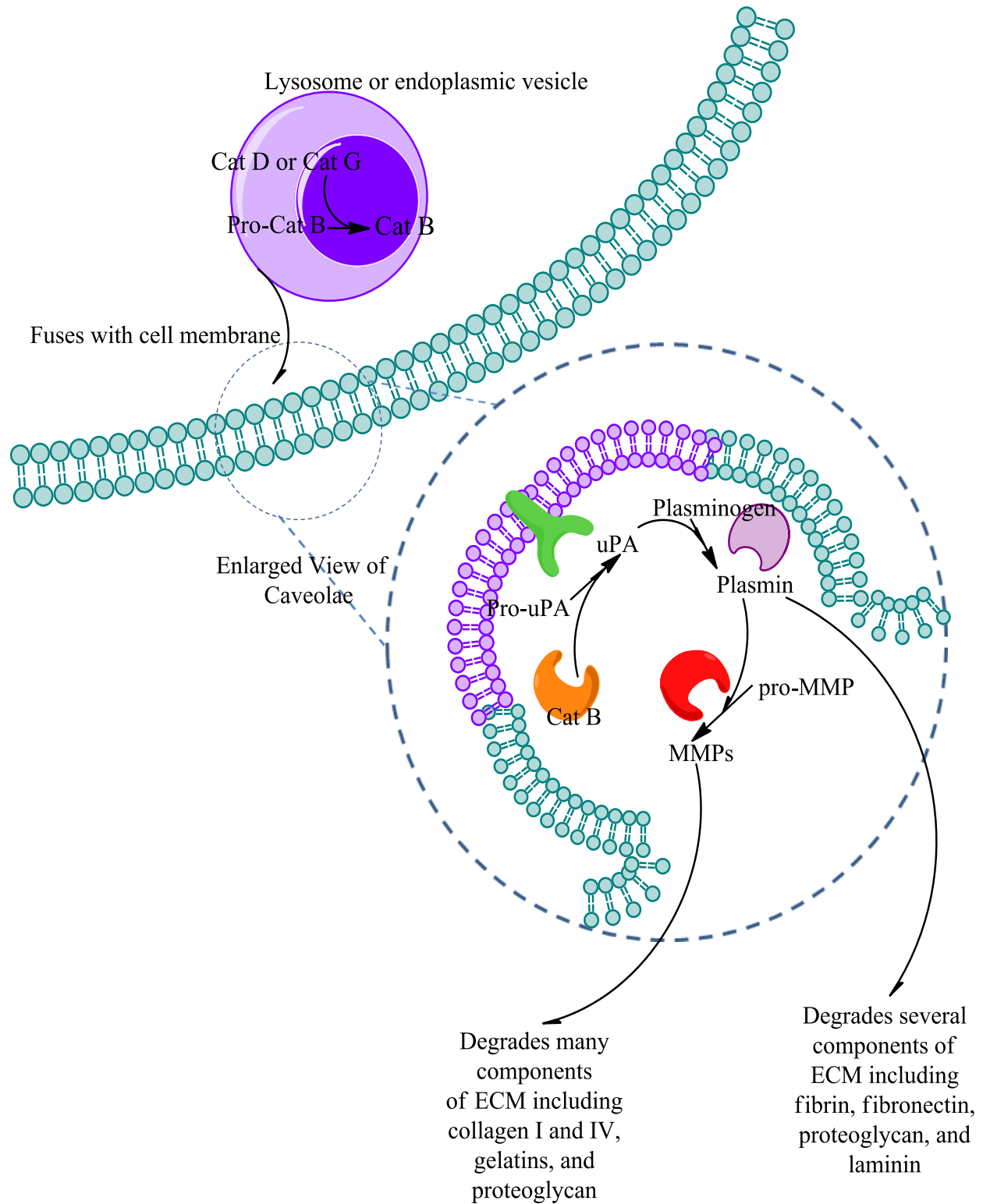
Figure 9 . Scheme of *in vitro* cathepsin B initiation of plasminogen cascade and
degradation of ECM

Activation of the plasminogen cascade can be described in a stepwise manner summarized below:[49]

1. Procathepsin B may be activated by cathepsin D or cathepsin G

2. Once activated, cathepsin B may activate pro-uPA which then converts inactive plasminogen to active plasmin. Plasmin degrades several components of the ECM such as fibrin, fibronectin, proteoglycans, and laminin

3. In turn, plasmin can activate matrix metalloproteinases (MMPs) which degrade components of the ECM such as collagen I and IV, gelatins, and proteoglycans

Introduction to Inhibitors of Cathepsin B

Because of the pathological implications with cathepsin B, cathepsin B has been a target molecule for different synthetic inhibitors. Although many *in vitro* studies have shown the effectiveness of inhibitiong cathepsin B *in vitro* to suppress tumor metastasis, no *in vivo* studies to date have proven the effectiveness of inhibition of cathepsin B as anticancer drugs.[50] Reasons include difficulty in designing an ideal inhibitor for the *in vivo* microenvironment. Likewise, designing an effective drug *in vivo* is difficult because knowledge is constantly expanding about the cellular function of proteases. For instance, matrix metalloproteinases inhibitors were successful in *in vitro* studies and had encouraging pre-clinical trial results. However, MMP inhibitors failed in advanced clinical trials because of severe side effects. Failure in later trials were caused by a lack of understanding towards the complex biology of the proteases such as all of their important cellular functions that are pro-survival.[49]

Ideal Inhibitor

The ideal pharmaceutical inhibitor is a small molecule that is completely selective for its target and is easily absorbed and distributed throughout the body, allowing the inhibitor to be effective at lower concentrations that are not dangerous to the body. Ideally, the drug should be available orally and can be used chronically.[50] Reversible inhibitors are also preferred over irreversible inhibitors because irreversible inhibitors have a higher chance of affecting off-target proteins and permanently blocking all the proteases that they bind to, leading to loss of the physiological function of the protease. Reversible inhibitors will more likely only partially inhibit the protease.[49]

Along with being small and reversible, ideally, an inhibitor would bind non-covalently to the active site since it is believed that non-covalent inhibitors provide better selectivity and cause less harmful effects than covalent inhibitors.[49] Likewise having fewer peptidic characteristics, increases the bioavailability of the compound. Bioavailability varies inversely with peptidic behavior because decreasing the peptidic characteristics lessens the likelihood of nonspecific degradation by endogenous protease inhibitors.

Current Inhibitors of Cathepsin B

Cathepsin B and possible inhibitors have been studied for over twenty years and many different drug designs have been created. In consequence, the first few sections will focus on some notable current inhibitors of cathepsin B found in literature.

Epoxysuccinyl Inhibitors

The epoxysuccinyl inhibitors are one of the most well studied inhibitors for cathepsin B. They are derivatives of the compound E-64, a compound isolated from *Aspergillus japonicas.*[51] Unfortunately, E-64 only displays marginal specificity for cathepsin B because of the conservation of active site residues among cysteine proteases. Almost all of these proteases have highly similar primary S2 substrate recognition pockets.[52] E-64 and its analogs bind irreversibly with Cys 29 in the S1 subsite of cathepsin B.[50] E-64 demonstrates an IC_{50} value of 55 nM with cathepsin B.

Although the IC_{50} value is low, E-64 is not a good candidate for pharmaceutical use because of its low permeability due to high peptidic nature. Esterification of E-64, making analog E-64d, has led to increased permeability. Although esterification makes the compound less active, esterification of E-64 has increased permeability and once inside the cell, the compound is hydrolyzed back into the active form.[50] Although esterification solves the problem of permeability, E-64 derivatives remain relatively nonspecific for cathepsin B.

CA074, is a E-64 derived compound that is specific for cathepsin B. The high specificity is attributed to interaction of CA074 with the two histidine residues located in the occluding loop of cathepsin B. However, the epoxy carbon of CA074 covalently binds to Cys 29.[53] Covalent inhibition is not desirable for clinical use because it leads to decreased selectivity, leading to inhibition of all targets due to irreversible nature of the mechanism of inhibition.[51]

Aldehyde Inhibitors

Aldehyde inhibitors have the ability to inhibit cysteine proteases through formation of a tetrahedral hemi(thio)acetal between the aldehyde and active site cysteine residue (Cys 29 in cathepsin B). Although the reaction is reversible, it involves the formation of a covalent bond. Aldehyde inhibitors inhibit cathepsin B in the lower micromolar range. However, they are peptidyl compounds and consequentially have a low permeability for the cell.

Non-peptidic Inhibitors

Compared to the abundance of peptidic inhibitors that have been studied over the past twenty years, far fewer non-peptidic inhbitors for proteases have been discovered and designed. Non-peptidic inhibitors have mostly been discovered by computational design and industrial screenings.[54]

Aryl Ureas and Aroyl Thoureas

Kinetic studies of aryl ureas and aroyl thoureas derivatives have shown that they all bind competitively and reversibly. Although these compounds inhibit cysteine proteases in general, they are more selective for protozoan enzymes over other cysteine proteases. Inhibition of cathepsin B by aryl ureas and aroyl thoureas is in the lower micromolar range.[53]

Organotellurium (IV)

Organotellurium (IV) compounds have high reactivities with cathepsin B that is attributed to the Lewis acid character of the tellurium atom.[50] Organotellurium (IV) binds

selectively and irreversibly to cathepsin B. The enzymatic activity can be reactivated after thiol treatment, indicating that the mode of inhibition involves oxidation of the active site cysteine.[53] Although oranotellurium (IV) compounds have high reactivities, they are only effective in the extracellular matrix. The intracellular matrix carries a large amount of reducing agents such as glutathione and NADPH that would render organotellurium ineffective.[50] A summary of selected current inhibitors discussed previously along with their associated IC_{50} values are summarized in Table 1.

Statement of Purpose
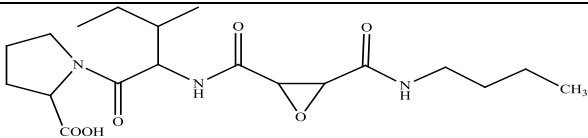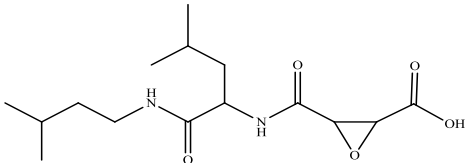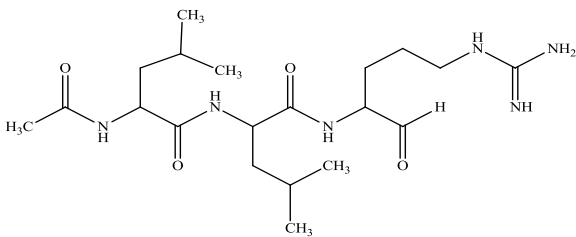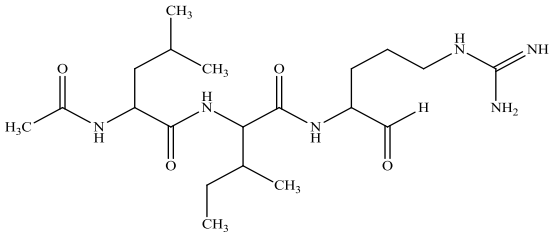
This study consistsof a collaborative project between the Trawick Biochemistry Laboratory and Pinney Organic Synthesis Laboratory at Baylor University. In a past study, many compounds containing a thiosemicarbazone moiety were found to be effective inhibitors of cathepsin L *in vitro.*[53]

Thiosemicarbazones (TSC) are a class of small molecular compounds that have been evaluated for the past fifty years for therapeutics against cancer and parasitical diseases.[55] [56] [57] They are attractive targets for drug design against cysteine proteases because they are small and possess no peptidic character and may be permeable to the cell, improving their bioavailability. Many of the thiosemicarbazone compounds were found to have low cytotoxicity levels to human cell lines, making them even more attractive for drug design. [58]

Because a number of thiosemicarbazone compounds were found to be effective against cathepsin L, the same library of compounds was tested against cathepsin B. Since cathespin B is a related cysteine protease, it is hypothesized that the TSC compounds may also effectively inhibit cathepsin B activity and may contribute to anti-cancer drug

24

design since this enzyme is upregulated in many cancers and is reported to play an important role in the metastasis of a number of cancers.

Table 1. Structure and IC50 value of selected inhibitors from literature for cathepsin B[50] [53]

Name	Structure	IC$_{50}$ (µM)
CA074		1.94
E-64c		8.70
Leupeptin		0.31
Acetyl-Leu-Ile-Arginal		0.15

CHAPTER TWO

Experimental procedure for the evaluation of potential inhibitors of cathepsin B for the treatment of cancer prevention

The data for the current research were collected from a series of research and experiments performed in partnership of the Trawick and Pinney laboratory groups in the Department of Chemistry and Biochemistry at Baylor University.

General Selection for Chemical Sources and Materials

The cathepsin B enzyme was purchased from Sigma (Lot # 110M1987) at a concentration of 4nM. The Z-Arg-Arg-aminomethylcoumarin (Z-RR-AMC) (Lot # 1007560) and Brij 35 were purchased from Sigma. The sodium phosphate was purchased from Sigma (Lot # 120K0125). The dithiothreitol (DTT) and ethylenediaminetetraacetic acid was purchased from OmniPur. The dimethyl sulfoxide used in this study was purchased from Acros Chemicals. A Thermo Fluoroskan Ascent FL microplate reader and black 96 well Corning 3686 assay microplates were used to perform the cathepsin B assays. Graphpad 5.0 software was used to analyze data received from Fluoroskan Ascent FL microplate such as for linear and non-linear regression of data. Distilled water that was further purified to 18Ω was used for assay. Micropipets used in this study were purchased from Eppendorf and the analytical balance used to weigh various compounds was a Mettler Toledo AX microbalance with an accuracy of 0.01mg.

Preparation of 100 mM Na₂HPO₄ buffer, pH 6.8

The sodium phosphate buffer pH 6.8 was prepared by weighing 10.65 g of sodium phosphate (Na_2HPO_4) (142.0 g/mol) and dissolving it thoroughly into a beaker with approximately 300 mL of ultrapure distilled water. Magnetic stir bar was used to facilitate dissolving. Homogenous mixture was transferred to a 500 mL volumetric flask and ultrapure water was carefully added to marker for a concentration of 150mM. The pH of the buffer was adjusted with phosphoric acid or NaOH to ensure that pH was 6.8 before each experiment.

Preparation of 40mM EDTA, Disodium Salt, dihydrate

The 40mM EDTA disodium salt dihydrate was prepared by weighing out 0.744g of EDTA disodium salt dehydrate (OmniPur lot# 3577B034) (372.24 g/mol) and dissolving it in a beaker with approximately 300 mL ultrapure water. A magnetic stir bar was used to facilitate dissolving. Once homogenous, the mixture was transferred into a 500 mL volumetric flask and filled carefully to the mark with ultrapure distilled water, making 40mM.

Preparation of assay buffer 1

Assay buffer 1 was prepared using 40mM EDTA, 100% DMSO, and 150mM sodium phosphate buffer according to Table 2.

Preparation of enzyme solution

Cathepsin B stock was prepared by diluting the 4 μL of cathepsin B into 0.1% Brij in a 1 to 20μL ratio. Thus 76μL of 0.1% brij was added to 4 μL of cathepsin B. To

27

prepare assay buffer 2 which is used to prepare the enzyme solution, DTT was added to buffer in a 4.63 mg of DTT to 10 mL of assay buffer 1. Enzyme solution was prepared according to Table 3. Enzyme is kept on ice to keep from denaturation

Table 2. Assay Buffer 1 Preparation

Total made (mL)	Na_2HPO_4(mL)	100% DMSO (µL)	EDTA(µL)
10	9.478	200	322
15	14.217	300	483
20	18.956	400	644
25	23.695	500	805

Preparation of Inhibitor of inhibitors

The library of thiosemicarbazone inhibitors were synthesized by the Pinney group at Baylor University. The stock solution of inhibitor was prepared by weighing out approximately 1 mg of dry compound and diluting it with 100% DMSO for a concentration of 20 mM. The mixture was fully vortexed to ensure that the compound was fully dissolved. Assay buffer 3 was prepared by diluting in a ratio of 9.678 mL of 150mM sodium phosphate buffer pH 6.8 to 0.322 mL of 40 mM of EDTA. Inhibitor solutions used for each experiment were prepared according to the serial dilutions in Table 4 and the dilutions made in Table 5.

Table 3. Enzyme solution preparation

Number of Columns	Cathepsin B Stock	Assay Buffer 2 (µL)
1	2.42	600
2	4.85	1200
3	7.27	1800
4	9.69	2400
5	12.12	3000
6	14.54	3600
7	16.96	4200
8	19.39	4800
9	21.81	5400
10	24.23	6000
11	26.66	6600
12	29.08	7200

Preparation of substrate solution

To make 8.970mM stock Z-RR-AMC, Z-RR-AMC was weighed and diluted in 100% DMSO using a 11.19 mg dry Z-RR-AMC to 2mL of 100% DMSO. The 8.970mM stock can be stored in a refrigerator and used to make a new substrate solution each day using Table 6.

Table 4. Serial dilution of stock inhibitors

Inhibitor Solution	Concentration (mM)	µL from previous solution	µL of 100% DMSO
A	20	------	-------
B	2	20	180
C	0.2	20	180
D	0.02	20	180
E	0.002	20	180
F	0.0002	20	180

Table 5. Preparation of inhibitor solution used for assay

Final Concentration (µM)	Concentration Made (µM)	Inhibitor Solution	(µL)	100% DMSO (µL)	Assay buffer 3 (µL)
15	45	A	1.1	8.9	490.0
10	30	B	7.5	2.5	490.0
5	15	B	3.8	6.3	490.0
1	3	C	7.5	2.5	490.0
0.5	1.5	C	3.8	6.3	490.0
0.1	0.3	D	7.5	2.5	490.0
0.05	0.15	D	3.8	6.3	490.0
0.01	0.03	E	7.5	2.5	490.0

Preparation of cathepsin B assay

Using the 10 – 1000 μL multichannel pipet, 50 μL of inhibitor solution or assay buffer 1 (for enzyme – substrate controls) was pipetted into the appropriate wells in the microplate. 50 μL of enzyme solution was then pipetted into the appropriate columns. The inhibitor – enzyme solution mixture was then incubated for 4 minutes and 55 seconds at 37°C for test to obtain IC_{50}, 0 minutes for progress curve test, and 5, 15, 30, 60, and 120 minutes for experiments that test the effects of pre-incubation time. After the incubation time, 50 μL of substrate solution was added to the each appropriate well as quickly as possible. The final concentration in each well is listed in Table 7. The reaction was read at E_x = 355 nm and E_m = 460 nm for 5 minutes. Data was analyzed on Graphpad 5.0.

Table 6. Substrate solution preparation

Columns	Stock (μL)	Water (μL)
5	61.2	3000
6	73.5	3600
7	85.7	4200
8	98.0	4800
9	110.2	5400
10	122.4	6000
11	134.7	6600
12	146.9	7200

Table 7. Final concentration in wells

Cathepsin B	2.0 nM
ZRR-AMC	60 uM
Buffer	100mM (Na Phosphate)
EDTA	1.25mM
DTT	1 mM
DMSO	2%
Brij	Minimal (8.3 e^-7 %)
pH	6.8

Protocol for IC$_{50}$ Test for Cathepsin B

This protocol tests for the IC$_{50}$ value of cathepsin B against an inhibitor. It requires running cathepsin B against inhibitor of varying concentrations, including a control with no inhibitor concentration.

1. Enzyme, inhibitor, and 60 μM substrate are prepared according to Table 2, 3, 4, and 5 in the general protocol section.
2. Enzyme and inhibitor are allowed to incubate for 5 minutes
3. Substrate is added and to each well and the experiment is run at an interval of 15 seconds with a measure count of 21 at excitation 355 and emission 460

Protocol for Progress Curves for Cathepsin B

Progress curves can give insight on the binding kinetics of an enzyme. For this test, inhibitor, substrate, and enzyme are run without any incubation time and tested for fifty minutes.

1. Enzyme, inhibitor, and 60 μM substrate are prepared according to Table 2, 3, 4, and 5 in the general protocol section.

2. Inhibitor, substrate, and enzyme are added to wells and test is run instantly at an interval of 3 seconds with a measure count of 1000 at excitation 355 and emission 460

Protocol for Reversibility Test for Cathepsin B

This protocol tests the reversibility of cathepsin B against an inhibitor with a known IC_{50} value. It requires incubation of inhibitor with cathepsin B which is tested against substrate in one-hundred fold excess.

1. Inhibitor is prepared according to Table 3 in general protocol and increased tenfold

2. A 1/10 dilution of cathepsin B at 4nM is used

3. Assay buffer 1 and assay buffer 2 is prepared according to general protocol

4. 60 μM substrate is prepared according to Table 5 in general protocol section and diluted one-third in Assay Buffer 1 and Assay Buffer 2

5. The enzyme solution is incubated with inhibitor solution at 37°C for one hour

6. 1.5 μL of the enzyme-inhibitor mixture is added to each respectively well

7. 148.5 μL of substrate mixture is added to each well and the experiment is run at an interval of 15 seconds with a measure count of 961 at excitation 355 and emission 460

Protocol for Competitive Test for Cathepsin B

To test whether inhibitor binds competitively, non-competitively, or with a mixed mechanism, cathepsin B is tested against varying inhibitor and varying substrate concentration in triplicate.

1. Enzyme and inhibitor is prepared according to Table 2, 3, and 4

2. Varying substrate concentration is prepared according to Table 8

Table 8. Serial dilutions for varying substrate concentration

Final Concentration(μM)	Stock Used (μM)	Volume of stock (μL)	Volume of 100% DMSO (μL)	Volume of Water (μL)
60.00	8970.00	80.27	-0.27	3920.00
40.00	180.00	2666.67	26.67	1306.67
20.00	120.00	2000.00	40.00	1960.00
6.00	60.00	1200.00	56.00	2744.00
0	0	0	80.00	3920.00

3.
4. Enzyme and inhibitor are allowed to incubate for 5 minutes

5. Substrate is added and to each well and the experiment is run at an interval of 15 seconds with a measure count of 21 at excitation 355 and emission 460

CHAPTER THREE

Results and Discussion for the Evaluation of Potential Inhibitors of Cathepsin B for the
Treatment of Cancer

Inhibition Studies with Thiosemicarbazones

This study was a collaborative project between Dr. Trawick's and Dr. Pinney's
research laboratory, which were responsible for the design, synthesis, and evaluation of
TSC derivatives as inhibitors of cysteine protease for the use in the arrest of cancer
growth and metastasis. Experiments conducted on cathepsin B contributed to significant
assay development for *in vitro* testing. Experiments were conducted to help elucidate the
mechanism of inhibition of TSC compounds with cathepsin B. The proposed general
view of nucleophilic attack mode of cysteine proteases such as cathepsin B is depicted in
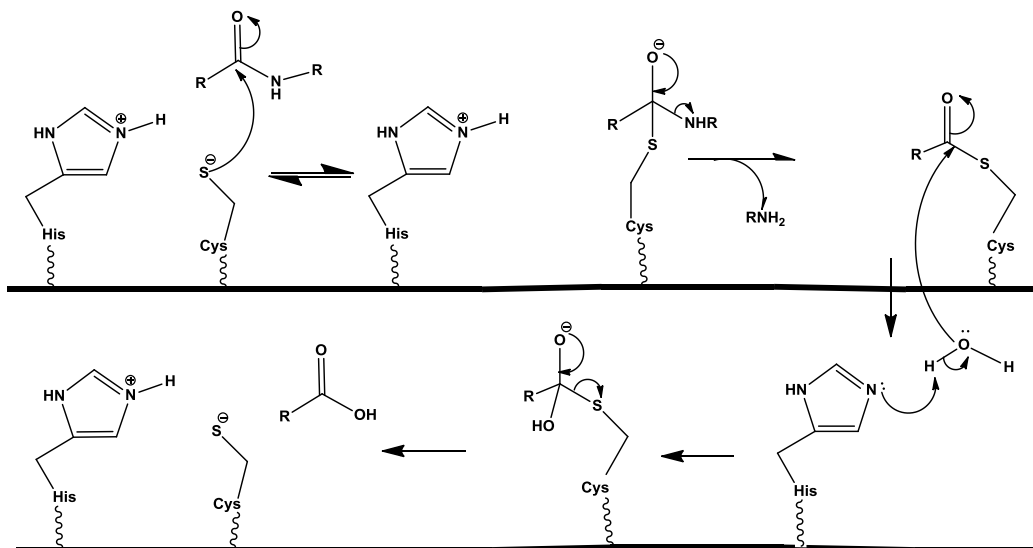Figure 10.

Figure 10. General view of nucleophilic attack mode of cysteine proteases

The general mechanism involves nucleophilic attack by the cysteine residue in the active site and protonation by the histidine residue. A transient covalent bond is then formed. The deprotonated histidine residue then acts as a base on water, deprotonating it. The deprotonated water then acts as a nucleophile that causes the dissociation of the covalent bond, resulting in formation of a carboxylic acid, loss of the amine group, and returned condition for the histidine and cysteine residues for another reaction.

EDTA disodium salt was added to act as a masking agent to sequester metal ions that would chelate with the active site thiolate ion. DTT prevented the formation of disulfide bonds in the active site. Brij, a non-ionic detergent, prevents the enzyme from aggregating on glass and plastic. DMSO, an organosulfur compound, makes nonpolar compounds more soluble in the final aqueous solution. Final conditions varied depending on the type of test being conducted. The inhibitors were tested in three stages to determine the potential mechanism of action (Figure 11).

The enzyme activity was monitored using benzyloxycarbonyl-L-arginyl-L-arginylalaninyl-7-amido-4-mtehylcoumarin (Z-RR-AMC) as the substrate. Once Z-RR-AMC was added to the solution, cathepsin B would cleave the peptidic bond in Z-RR-AMC, releasing a fluorescent 7-amino-4-methylcoumarin product and a non-fluorescent Z-RR product (Figure 12). The amount of fluorescent 7-amino-4-methylcoumarin (AMC) produced was monitored over time and measured as relative fluorescent units (RFU). For this study, the rate of AMC produced was equivalent to the initial velocity of cathepsin B.
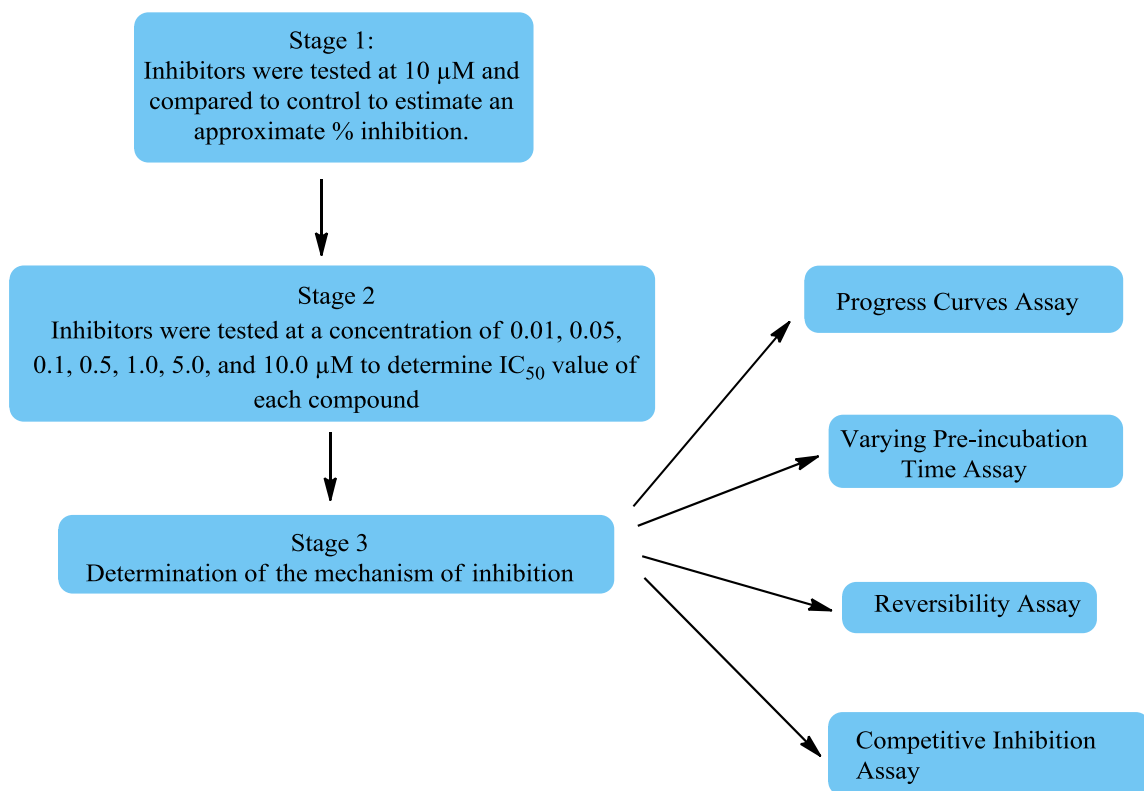
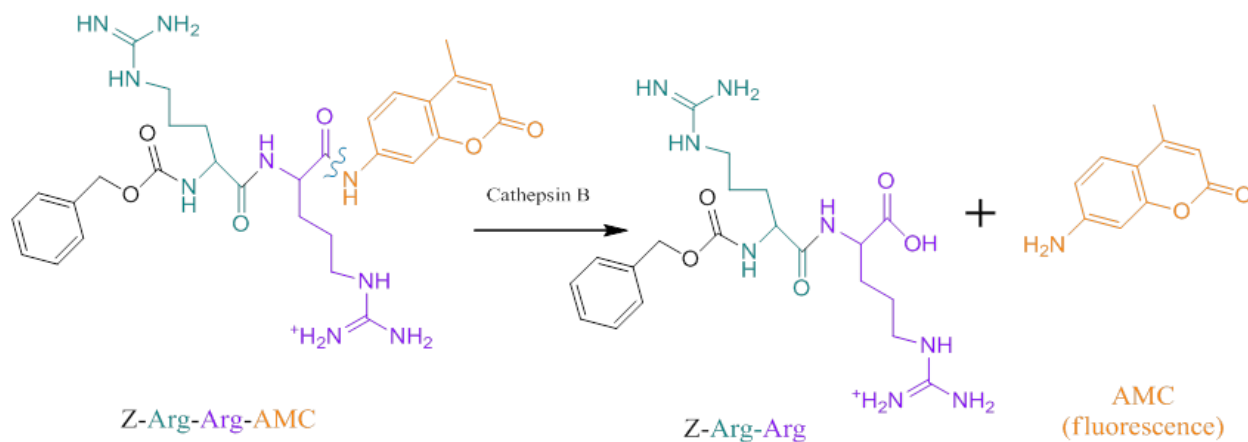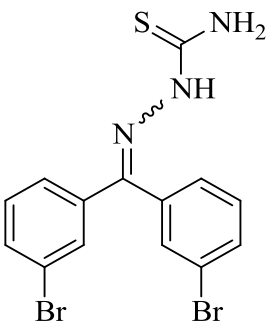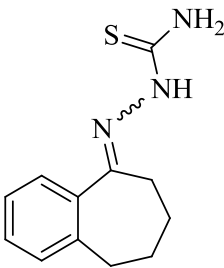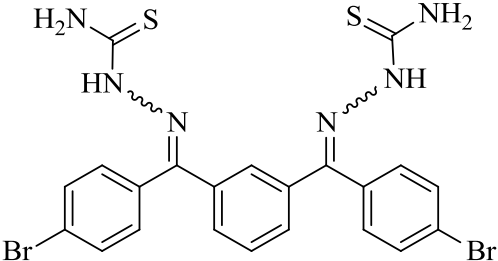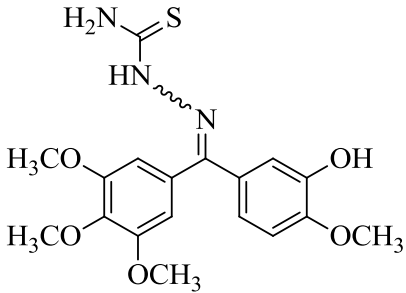Figure 11. Schematic depiction of methods used to analyze inhibitor-enzyme relationship

Figure 12. Hydrolysis of Z-RR-AMC by cathepsin B. The fluorescent AMC product produced after cleavage of the amide bond by cathepsin B is measured as relative fluorescence units as a function of time

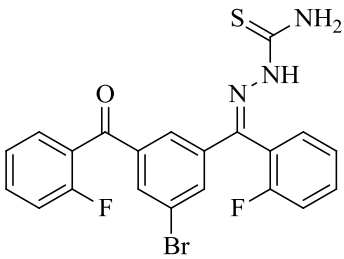*Stage One: Determination of Inhibitory Activity*
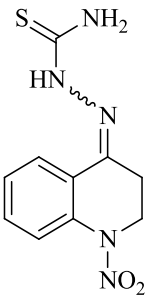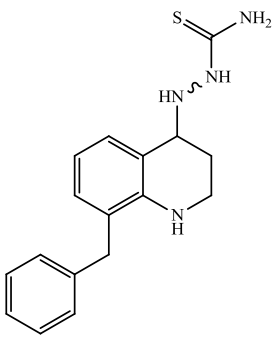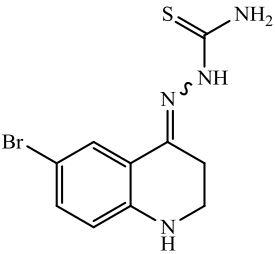
For stage one, thirteen compounds were tested to determine the inhibitory activity of the compound at 10 µM cutoff. Stock solutions of 20 mM were dissolved in DMSO and further diluted to 10 µM. Inhibitor was pre-incubated with cathepsin B for five minutes before adding Z-RR-AMC, a fluorogenic substrate. The reaction was monitored using a fluorescent microplate reader at an excitation wavelength of 355 nm and an emission wavelength of 460 nm at 37°C for five minutes. The final assay conditions were 2.0 nM cathepsin B, 60 µM Z-RR-AMC, 100 mM sodium phosphate buffer, 1.25 mM EDTA, 1 mM DTT, 2% DMSO, pH 6.8, and minimum Brij.

Percent inhibition was obtained by comparing the velocity obtained with 10 µM of inhibitor to the velocity obtained using zero inhibitor, the control. Six of the compounds were tested in sextuplicate and the other ten were tested in triplicate. Results are summarized in Table 9 and Appendix A. The cutoff value to determine whether the inhibitor was a hit or not was at least 50% inhibition when using 10 µM. Thus, compounds with a percent inhibition approximately 50% or more were tested further. If compounds had an inhibitory activity of less than 50% when using 10 µM, the compound would require more than 10 µM to inhibit 50% of the enzyme activity, meaning the compound has less than satisfactory inhibitory effects. Out of the sixteen tested compounds, two were further tested and proceeded to stage 2.

Table 9. Determination of inhibitory activity

Compound	Structure	% Inhibition ± standard deviation
1		89.45 ± 2.734
2		8.360 ± 5.005
3		4.641 ± 1.490
4		93.13 ± 0.9757

Compound	Structure	% Inhibition ± standard deviation
5		12.88 ± 2.384
6		52.94 ± 2.561
7		46.40 ± 3.340
8		20.75 ± 2.867
9		31.08 ± 0.675

Compound	Structure	% Inhibition ± standard deviation
10		10.71 ± 1.335
11		10.57 ± 5.691
12		22.50 ± 1.735
13		40.96 ± 2.717

Stage Two: Determination of IC$_{50}$

In stage, the IC$_{50}$, or concentration required to achieve half saturation of the enzyme, was obtained. The IC$_{50}$ value is a useful tool to compare and rank the effectiveness or potency of hits validated in stage 1.

Although the IC$_{50}$ value is a very useful tool for analyzing data, it is easily perturbed by changes in solution such as a change in pH, ionic strength, temperature, enzyme concentration, and pre-incubation time. Thus to avoid bias caused by changes in solution, the same assay conditions were used to test the three validated hits. Each experiment was performed as follows: stock solutions (20 mM) of each of these non-polar inhibitors were dissolved in DMSO. Dilutions were prepared with varying concentrations of inhibitor and water, resulting in inhibitor concentrations of 0.01, 0.05, 0.1, 0.5, 1.0, 5.0, and 10.0 µM. The reaction was monitored at an excitation wavelength of 355 nm and an emission wavelength of 460 nm at 37°C for five minutes (Figure 13). The final assay conditions were 2.0 nM cathepsin B, 60 µM Z-RR-AMC, 100 mM sodium phosphate buffer, 1.25 mM EDTA, 1 mM DTT, 2% DMSO, pH 6.8, and minimum Brij.

The results were fitted to a model (Equation 1) by non-linear regression using Graphpad 5.0 software, and the IC$_{50}$ values were determined. Average of the triplicate IC$_{50}$ values were used for analysis.

$$\frac{v_i}{v_0} = v_i + \frac{(v_0 - v_i)}{1 + 10^{\log(IC_{50} - x)Hillslope)}} \qquad \text{Equation 1}$$

The two compounds showed comparable inhibition (IC$_{50} \leq 5$ µM). Hits were tested multiple times to verify their reproducibility.
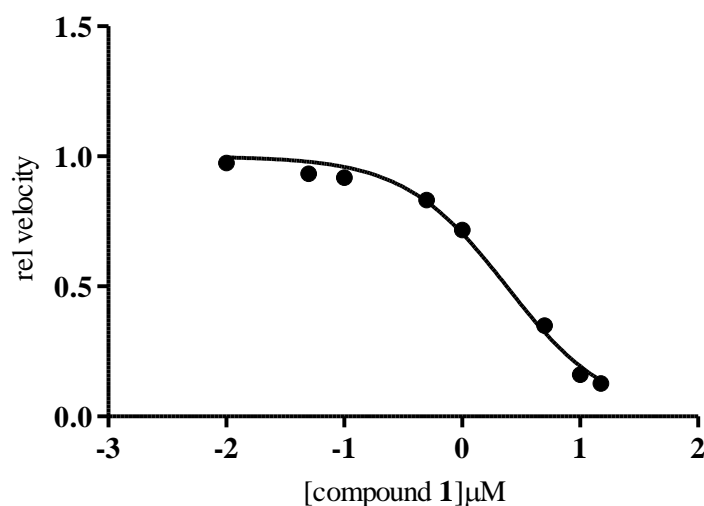
Figure 13. IC50 curve of compound **1** fitted to dose-response curve

Stage 3. Determination of Mechanism of Inhibition

Progress Curves

The progress curves of a compound gives insight into whether or not a compound binds quickly or slowly. The progress curve assay is similar to the IC_{50} curve assay but the reaction is monitored for three hours instead of five minutes. Thus the final assay conditions were 2.0 nM cathepsin B, 60 µM Z-RR-AMC, 100 mM sodium phosphate buffer, 1.25 mM EDTA, 1 mM DTT, 2% DMSO, PH 6.8, and minimum Brij.

The hallmark of slow inhibition is that the degree of inhibition at a fixed concentration will vary as equilibrium is established. Thus a different slope will exist for the initial velocity and the steady state velocity which develops as the equilibrium is established between the free and bound enzymes On the other hand, the progress curve of the uninhibited reaction will be linear.

Figure 14. Progress curve of compound **1** at 10 µM that displays two distinct slopes
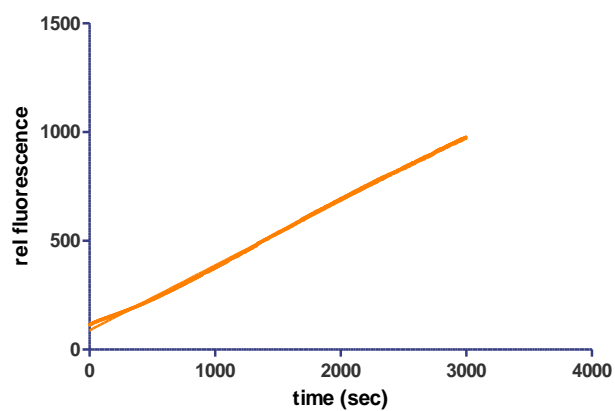
Figure 15. Progress curves of uninhibited reaction. Displays a linear trend with an r2 fit of 0.999.
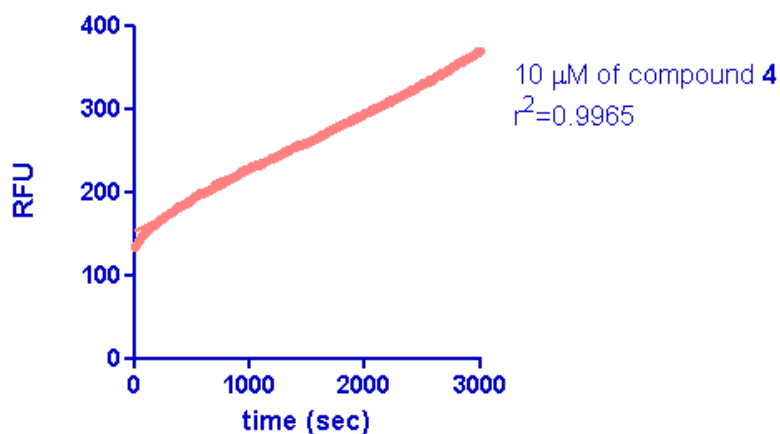
Figure 16. Progress curve of compound **4** at 10 µM

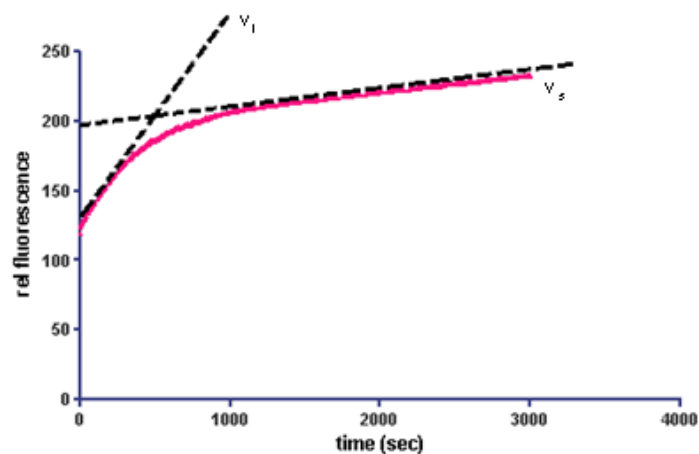As shown in Figure 14, compound 1 displays the characteristics of a slow binding inhibitor. The progress curves of compound **1** at 10 μM displays two distinct slopes, a steeper slope during the initial reaction and a much less steep slope during the steady state of the reaction. Figure 16, on the other hand shows that compound **4** does not bind slowly because the progress curves is linear just like the progress curves of the uninhibited reaction in Figure 15. Figure 17 shows the progress curve of compound **1** at varying inhibitor concentrations.
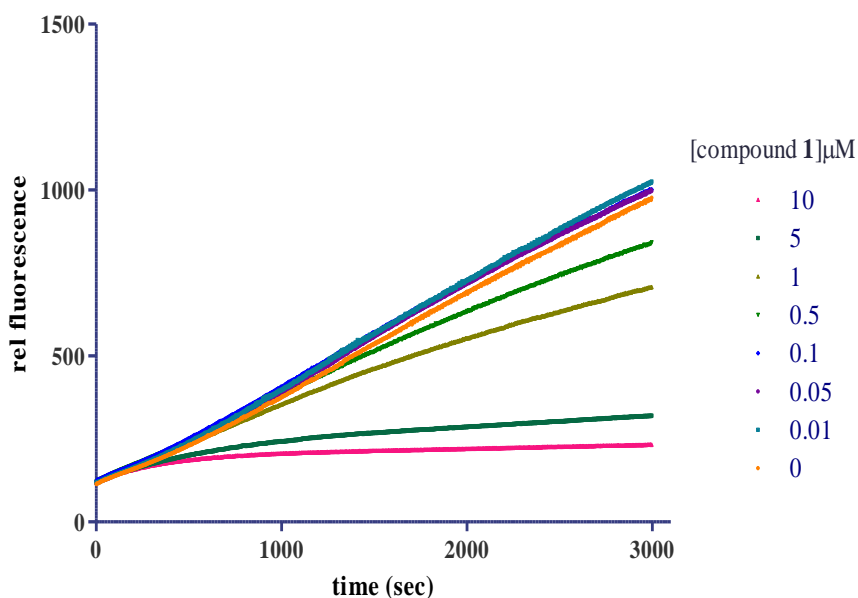
Figure 17. Progress curves of compound **1** with varying inhibitor concentrations (10, 5, 1, 0.5, 0.1, 0.05, 0.01, and 0 μM)

Varying Pre-Incubation Times

Because compound **4** had linear progress curves that did not vary with time, compound **4** most likely binds in a time independent, classical competitive inhibition mechanism. However, because compound 1 binds slowly and has varying slopes as time progresses, the compound binds in a time dependent fashion. Figure 18 shows that as pre-

incubation time of the enzyme and inhibitor increases the IC_{50} value decreases. This trend coincides with the fact that the enzyme eventually reaches steady state equilibrium between bound and unbound enzyme.
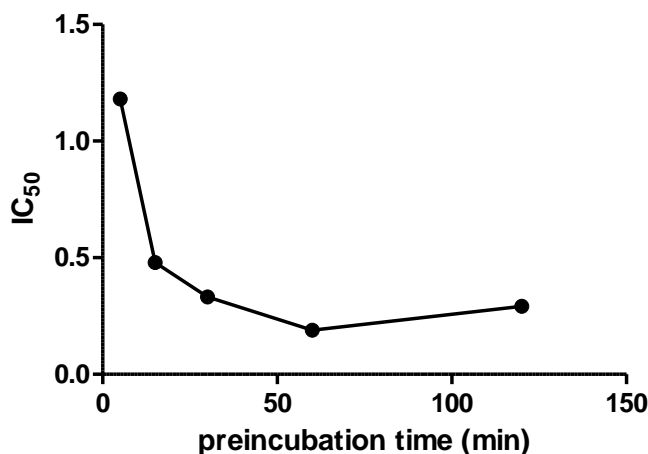
Figure 18. Time dependent $IC_{\neg 50}$ of compound **1**

Reversibility Assay:

To determine whether or not the inhibitor bound reversibly or irreversibly, the recovery of enzymatic activity was measured and monitored after rapid and large dilution of the inhibitor-enzyme complex. The enzyme was used at a concentration of 100-fold times the concentration required for assay activity. In this case, the enxyme used was 0.4 nM. The enzyme was incubated with a concentration of inhibitor that is 10-fold the IC_{50} value. After an hour of incubation at 37°C, the mixture is diluted 100-fold into reaction buffer containing the enzyme substrate Z-RR-AMC. The reaction was run at an excitation of 355 nm and emission wavelength of 460 nm for four hours. The result for the reversibility assay for compound **1** and compound **4** are summarized in Figure 19 and 20.

46
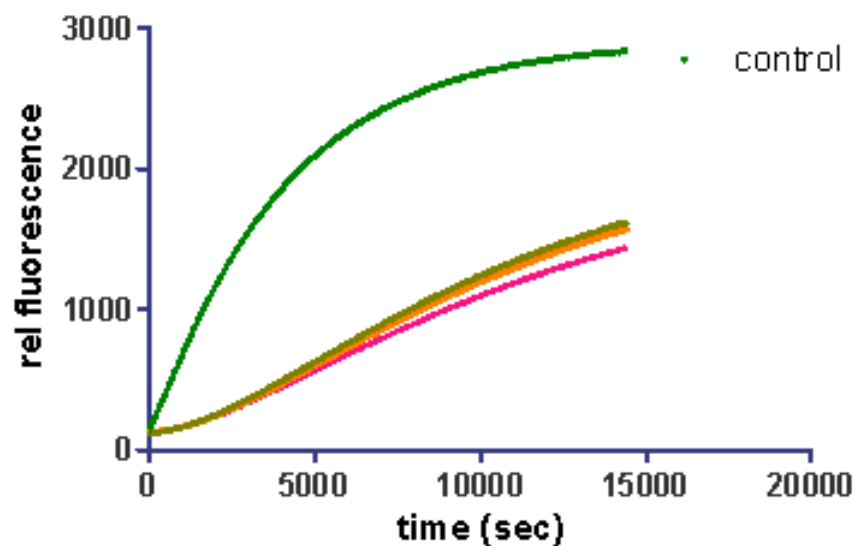
Figure 19.Reversibility curves for compound **1**
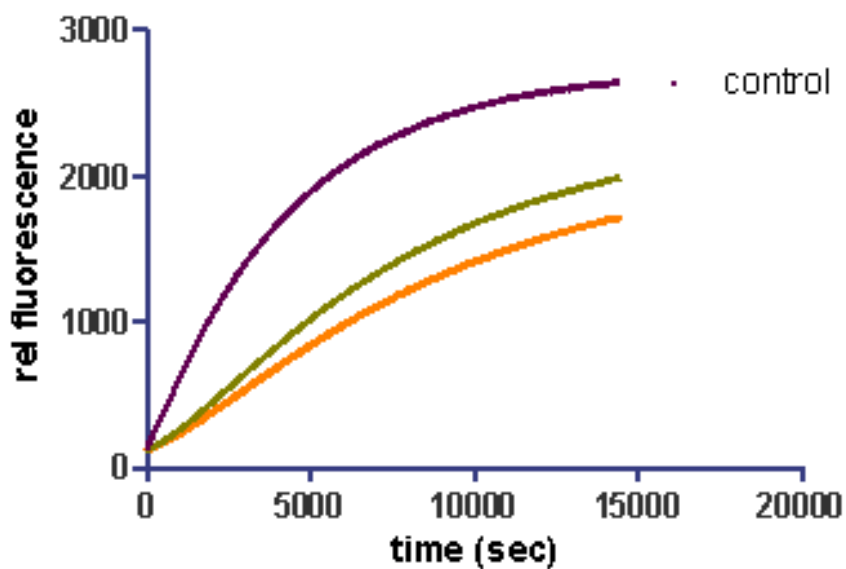
Figure 20. Reversibility curves for compound **4**

The progress curves obtained from the reversibility assay were then compared to the progress curve of cathepsin B in in the absence of inhibitor (control). The reversibility progress curves for both compound **1** and compound **4**, are not linear, meaning that the inhibitor is not rapidly reversible. Instead, the curves are curvilinear,

47

with a lag phase that has a concave curvature followed by an approximately linear trend. The curvature of the progress curve reflects the slow recovery of activity as the inhibitor slowly dissociates from the enzyme's active site, causing the lag in linearity.

The difference between the RFU of compound **1** as compared to its control is greater than the difference between the RFU of compound **4** and its control, indicating that compound **1** is more slowly reversible than compound **4**. During the lag phase of Figure 15, the slope is much less steep than the slope of the control. On the other hand, the slope of compound **4** is less steep during its lag phase, indicating that the inhibitor is reversible but dissociates faster from the active site than compound **1**.

Modality of Inhibition: Competitive Inhibition

The competitive inhibition assay consists of testing varying concentration of inhibitor and varying concentration of substrate with a constant amount of enzyme. The results are plotted with velocity of the reaction with respect to concentration of substrate. Using Graphpad 5.0, the data were fitted to a non-linear regression model. (equation 2)

$$v = \frac{V_{max}[S]}{[S] + K_M\left(1 + \frac{[I]}{K_i}\right)} \qquad \text{Equation 2}$$

Both compound **1** and compound **4** fitted the model well, indicating that the two compounds exhibit competitive inhibition. Compound **4** was transformed into a Lineweaver-Burk plot (Figure 23). The lines of the double reciprocal plot intersect at the y-axis, indicating that the mode of inhibition is most likely competitive.
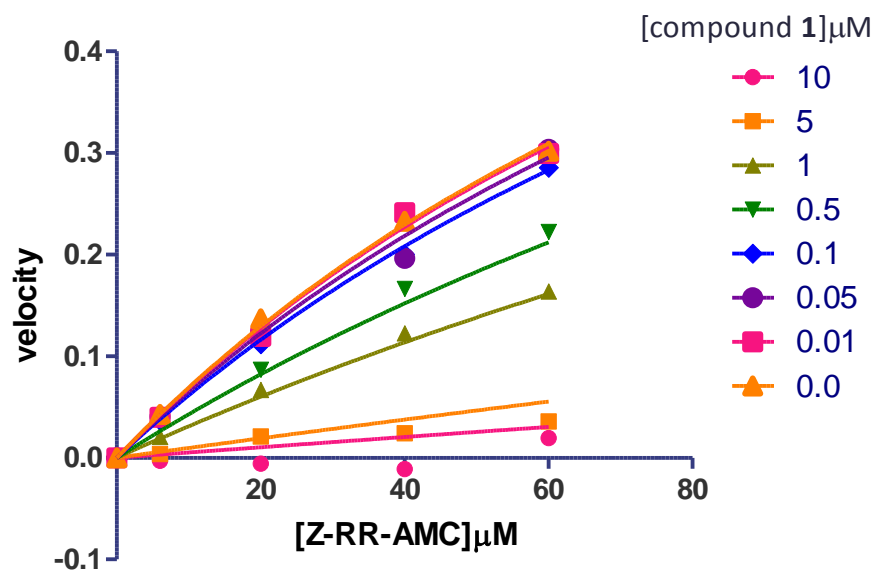
Figure 21.Substrate titration of steady state velocity for an enzyme in the presence of compound **1** at varying concentration. Untransformed data
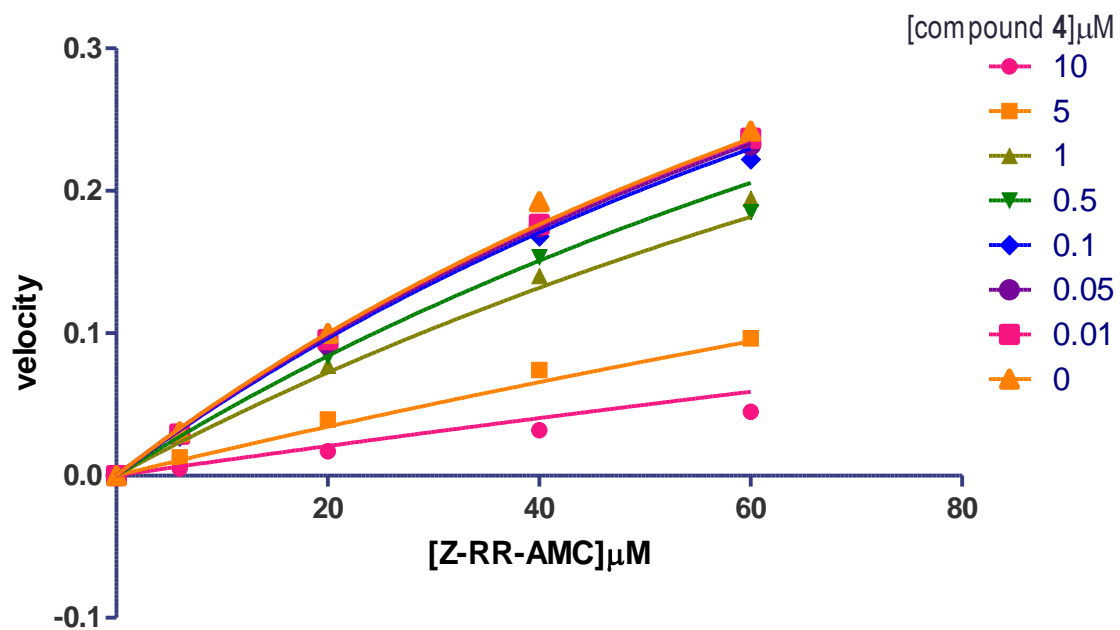
Figure 22. Substrate titration of steady state velocity for an enzyme in the presence of compound **4** at varying concentration. Untransformed data
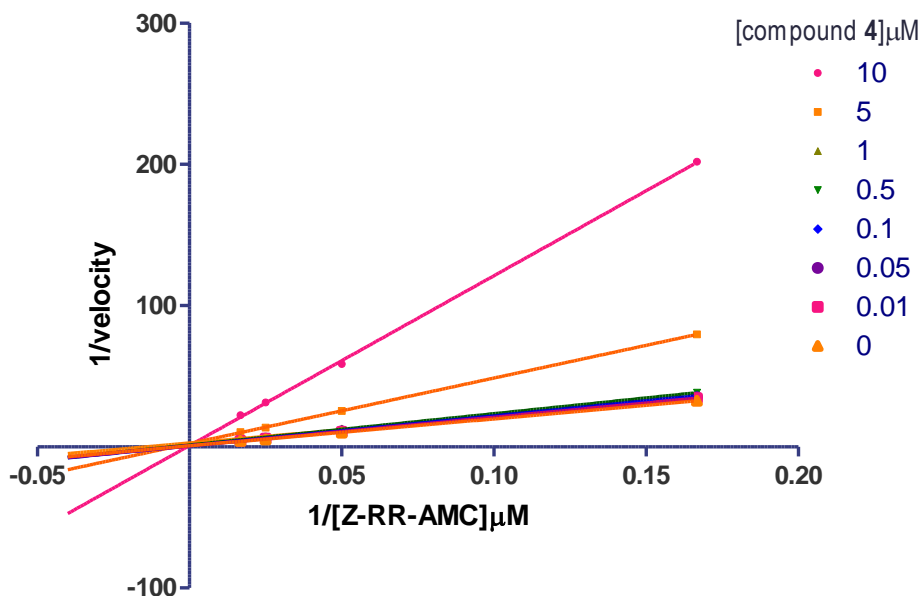
Figure 23. Double reciprocal (Lineweaver-Burk) plot of compound **4**

Discussion of the Thiosemicarbazones as Inhibitors of Cathepsin B

Table 10 summarizes the results from this research. The benzophenone thiosemicarbazone, compound **1**, from the library tested, was previously reported as a comparable non-peptidic inhibitor of cathepsin B with an IC_{50} of approximately 2 μM. In this study, the mechanism of inhibition of compound **1** was further tested. Likewise fifteen other compounds were evaluated and compared to compound 1. Out of the fifteen newly tested samples, compound **4** showed satisfactory inhibition efficacy. The mechanism of compound **4** was likewise further tested.

A comparison of compound inhibitory activity at 10 μM reveals a trend that having an electron donating or activating group on the aromatic ring in the meta-position contributes to more efficient inhibitory activity. Compounds **1** contain two bromide groups at the meta position, and compound **4** contains four methoxy groups in the meta and para-positions and a hydroxyl group in the meta-position. Compound **5** on the other

50

hand, had two deactivating or electron withdrawing groups in the meta-positions and exhibited a much smaller percent of inhibition at 10 μM than compounds **1** and **4**. Compound **6** which resembles compound 1 except that one meta-position substituent is an acetic group instead of a bromide, exhibited significantly less inhibitory activity than compound **1**. (Compound **6** was further investigated in another study) The loss of inhibitory efficacy may be due to the slightly electron withdrawing effects of the carbonyl of the acetic group.

Comparison of the compounds inhibitory activity at 10 μM also showed a trend that more bulky thiosemicarbozones (containing more than two aromatic rings) were less successful at inhibiting cathepsin B activity. None of the bulky (containing more than two aromatic rings) displayed more than 50% inhibitory activity at 10 μM.

Future studies on cathepsin B could consist of testing more thiosemicarbozones that are not bulky and that contain electron donating groups in either the meta or para-positions. Compounds with electron donating groups in the ortho-position were not tested in this study and should be tested in future studies.

The thiosemicarbazone's mechanism of inhibition was also studies. As summarized in Table 10, compound 1 binds in a time dependent, slow, tight, reversible and competitive manner. Compound binds in a similar manner, but is not time dependent.

Table 10. Summary of Results

Compound	IC$_{50}$ (μM)				Mode of Inhibition
1	1.64±0.656	Slowly Reversible	Time Dependent	Slow tight binding	Competitive
4	2.86±0.179	Rapidly Reversible	Not time Dependent		Classically Competitive
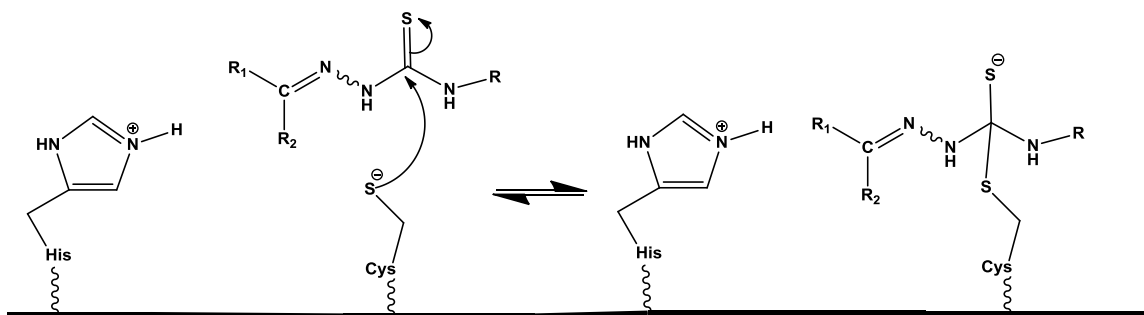
Figure 24. Proposed mechanism of inhibition of compound **1**

Figure 24 shows the proposed mechanism of action that thiosemicarbazones such as compound **1** and compound **4** undergo when inhibiting cathepsin B. The proposed mechanism of inhibition involves a nucleopilic attack by the cysteine residue and formation of a transient covalent bond. The transient covalent bond then collapses back towards the beginning reagents in a reversible manner.

Slow off-rate inhibitors such as compound 1have a significant clinical advantage over rapidly reversible inhibitors because the activity of the bound target enzyme is effectively shut off for a significant time period. This would reduce the time of high compound levels in circulation that may potentially lead to reducing the likelihood of off-target toxicity.

Competitive inhibitors such as compound **1** and **4** are also potentially useful clinically. Drugs in clinical use today such as Methotrexate, Lovastatin, Pravastatin, and Gleevec function as competitive enzyme inhibitors.[59] Knowledge about the mode of inhibition can also lead to mechanism based drug design that mimics the substrate, transition state, or product.

In conclusion compounds **1** and **4** needed less than 5 μM to inhibit approximately fifty percent of enzyme activity, indicating that thiosemicarbazones have the potential to

serve as effective inhibitors of cathepsin B and may be used clinically to decrease protein turnover, tumor progression, apoptosis and angiogenesis. Future studies may include testing the *in vivo* ability of compound **1** and compound **4** in cell based assays and determining the cytotoxicity of compounds **1** and **4**.

CHAPTER FOUR

Statement of Purpose and Significance of the Study of Cruzain

Introduction to Chagas' Disease

Chagas' disease is named after the Brazilian physician Carlos Chagas who discovered the disease and published his findings in 1909.[60] It is caused by the protozoan parasite *Trypanosoma cruzi.*[61] Chagas' disease is endemic in almost all Latin American countries, including countries in Central America such as Mexico and countries in South America such as Brazil.[59] Chagas' disease causes more deaths than any other parasitic disease in the Americas.[62] Approximately 8 million people are infected with *Trypanasoma cruzi*, resulting in approximately 50,000 deaths per year.[63]

Although the insect vectors are found predominantly in rural regions where housing is made from material such as mud, adobe, straw, and palm thatch, Chagas' disease is not limited to rural regions. Large scale movement from rural areas to urban areas throughout Latin America and the world have led to an increased distribution of Chagas' disease.[64] It is estimated that between the years 1981 and 2005, approximately 89 to 700 thousand Latin Americans infected with *T. cruzi* parasite migrated to the United States (Figure 25).[65]

The most common insect vector is the triatomine bug (Figure 26). The triatomine insects, commonly known as the "kissing bugs" because of their preference to bite faces, become infected when they bite an infected animal or human. During the day, the triatomine bug hides in crevices in the roofs and wall. However at night, the bugs feed on people's faces.[62] After feeding, the bugs ingest the blood and defecate on the person. If

the parasitic feces come into contact with mucous membrane or a break in skin such as when a person unknowingly scratches their face at night, the person becomes infected.[32]

A person may also become infected by other means such as transmission from an infected mother to her unborn baby, consumption of uncooked food from meat infected by infected feces, blood transfusion, organ transplantation, or exposure in the laboratory.[52] Although the triatominae bug is the most common vector mode of transmission, other animals in the United States such as raccoons, opossums, armadillos, and rural dogs have all been shown to be infected by *T. cruzi.*[60]

Figure 25. Eleven different species of triatomine bug have been reported in the Southern United States[66] (Fig. was taken directly from http://www.cdc.gov/parasites/chagas/gen_info/vectors/index.html)

Figure 26. Triatoma gerstaeckeri, a species of triatomine bug found in Southern United States, put next to a penny for scale. (Photo courtesy S. Kjos.) [61] (Fig. was taken directly from http://www.cdc.gov/parasites/chagas/gen_info/vectors/index.html)

Pathology of Chagas' Disease

The life cycle of *T.cruzi* can be summarized as follows (Figure 27). First, the reduviid bug has a mixture of *T. cruzi* morphologies which passes into the midgut. In the midgut, the *T. cruzi* morphologies differentiate into amistigotes. Within the midgut, amistigotes replicate and eventually transform into epimastigotes which swell and extend out flagella. Elongated epimastigotes attach via hydrophobic interaction to the waxy cuticle along the walls of the hindgut where they differentiate into the metacyclic form. Once matured, the metacyclic forms detach from the cuticle and are excreted. The excreted metacyclic form of *T.cruzi* can then infect a human by entering through a cut or break in the skin. Once inside, the cells transform back to amastigotes where they infect tissue and multiply using binary fission. Eventually, the intracellular amastigotes burst out of the cell and infect other tissue after entering into the blood stream.[67]

Chagas' disease can be distinguished into three phases: acute, indeterminate, and chronic. The acute phase is characterized by high tissue and blood parasitic involvement and 5% myocarditis incidence. Its symptoms tend to be nonspecific. The indeterminate phase is a patient who is positive for *T. cruzi* infection but does not show any symptoms. The chronic phase which normally occurs 10 to 30 years after infection is characterized by approximately one-fourth of infected population manifesting ventricular arrhythmias, bradiarrhythmias, and other heart problems.[60] Because of the potentially long asymptomatic phase, Chagas' disease is a silent killer once reactivated after many years of silently infecting various tissues in the body.[58]

Current Treatment for Chagas' Disease

Currently there are two drugs that treat *T. cruzi* infection, benznidazole and nifurtimox (Figure 28).[59] Both drugs work by shortening the acute phase of *T. cruzi*. However the drugs are unsatisfactory and only cure fifty percent of patients treated with either drug and also cause substantial amounts of side effects and lead to high amounts of toxicity and are not accepted by the United States FDA.[59] [61] Both drugs are also ineffective in the chronic determinate phase of Chagas' disease. In addition increasing resistance to both compounds have increased treatment failure.[68] Antiparasitic drugs in the acute phase have approximately 50 to 80% chance of being successful.[69] The chances of successful treatment range from 20-60% in the indeterminate or asymptomatic phase.[67] There is no current cure for Chagas' disease once it is well established.
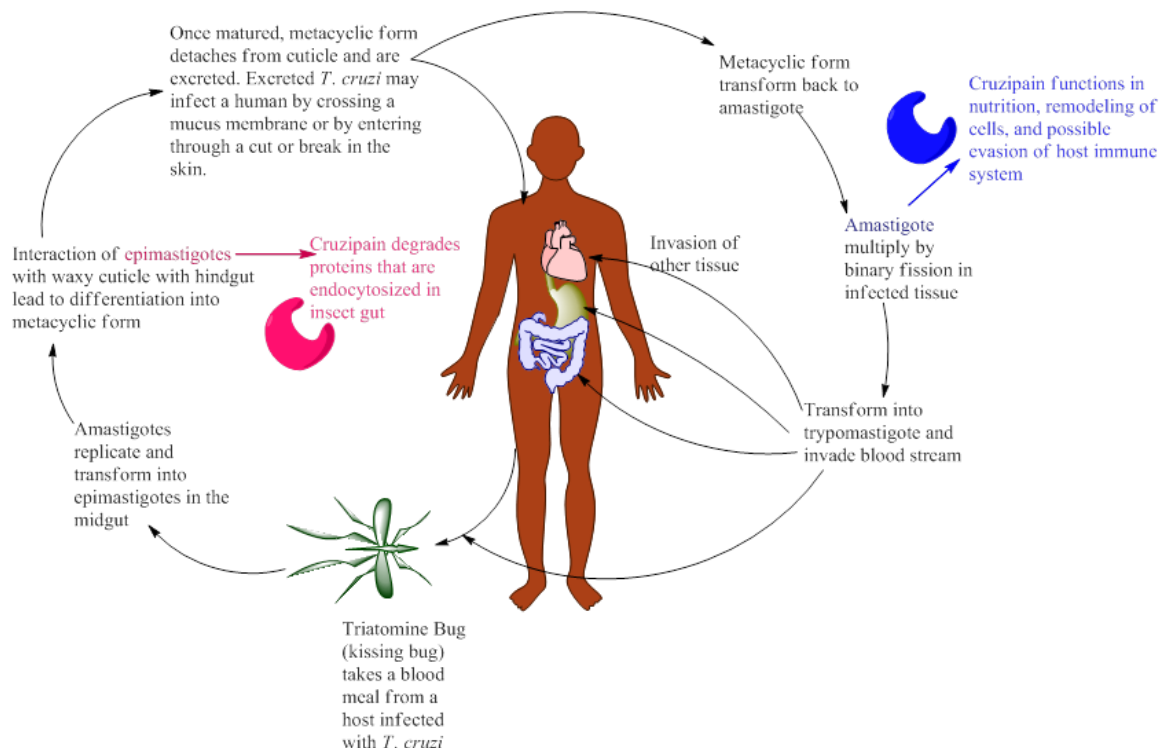

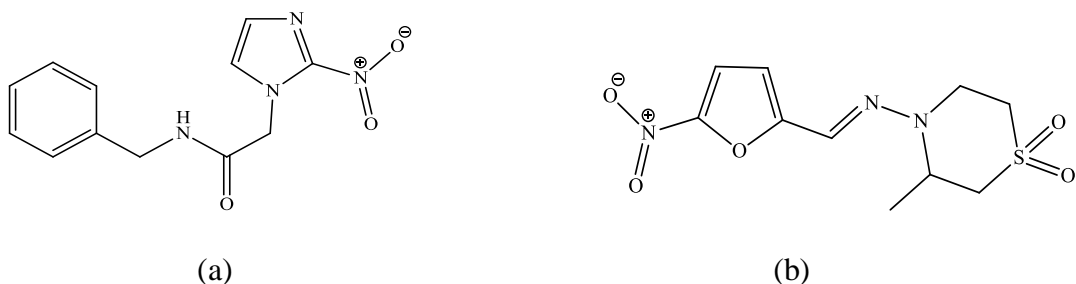
Figure 27. Cartoon depiction of lifecycle of *T. cruzi*

Figure 28. (a)Structure of benznidazole (b) Structure of nifurtimox

There have been initiatives to knockdown transmission rates by vector control such as the "Southern Cone" initiative.[58] In fact, vector control and closer screening of blood banks since 1991 has decreased the number of people infected with *T. cruzi* from 18 million to 8 million.[61] Some success has been found in Brazil, Uruguay, and Chile, primarily through the spraying of insecticides on houses to kill the vector *Triatoma infestans.*[58] However, in some areas where Chagas' disease is endemic such as Mexico, no such program has been initiated.

Likewise vector control requires constant spraying which promotes the insect's resistance to current pesticides.[58] Such a case of increased insect resistance has occurred in Argentina.[58] Alternative insecticides are available but many have issues concerning increasing toxicity to humans and the environment.[58] Improving houses to make them less attractive to the "kissing" bugs have also been proposed; however, the costs of such improvements are not feasible for developing countries to sustain.[58]

Different Approaches to Chagas' Disease Chemotherapy

Some current chemotherapy approaches include inhibitors that target DNA topoisomerase such as antracyclines, camptothecins, and fluoroquinolones which have all been screened for inhibitory activity against the typomastigote phase of *T. cruzi.*[70] [71] Other inhibitors are being designed to inhibit sterol biosynthesis in *T. cruzi.* Sterols are

required for maintenance of the cell membrane in *T. cruzi*. Some compounds such as squalene synthase inhibitors and squalene epoxidase inhibitors have been tested *in vitro* for their ability to inhibit sterol biosynthesis. Unfortunately, these inhibitors may potentially be dangerous to human host by inhibiting a similar pathway for sterol synthesis in humans.[72][73]

Thiosemicarbazones as potential therapeutic drug

Thiosemicarbazones were tested as a validated target for *T. cruzi* infection in a study in 2002 by Du *et al.*[74] Du *et al* tested over 100 thiosemicarbazones as inhibitors against the parasitic cysteine protease cruzain, a recombinant form of cruzipain.[70] Cruzipain is the actual enzyme found in *T. cruzi*. Cruzipain contains a 130 amino acid C-terminal extension that is not present in the recombinant form cruzain (Figure 29). Natural cruzipain is a mixture of isoforms. No large differences in kinetic parameters have been observed between cruzain and cruzipain.[75]

Cruzipain (Figure 30) is an appealing target for parasitic chemotherapy. It is a cathepsin L like cysteine protease, falling into the same family as papain. It has a conserved active site catalytic triad (cysteine, histidine, and asparagine residues) that characterizes papain like cysteine proteases. Cruzipain is expressed in all life cycle stages of the parasite. During the epimastigote stage it functions in degradation of proteins that are endocytosized from the insect gut.[70] During the amastigote stage, cruzipain is in both the lysosome and on the surface of the parasite, functioning in nutrition, remodeling of mammalian cell and potential evasive defense against host immune system.[70] Cruzipain has also been found to be essential to replication of intracellular parasite.[70] *T. cruzi*

infected mouse models have effectively been cured after treatment with a cruzipain inhibitor.[70]
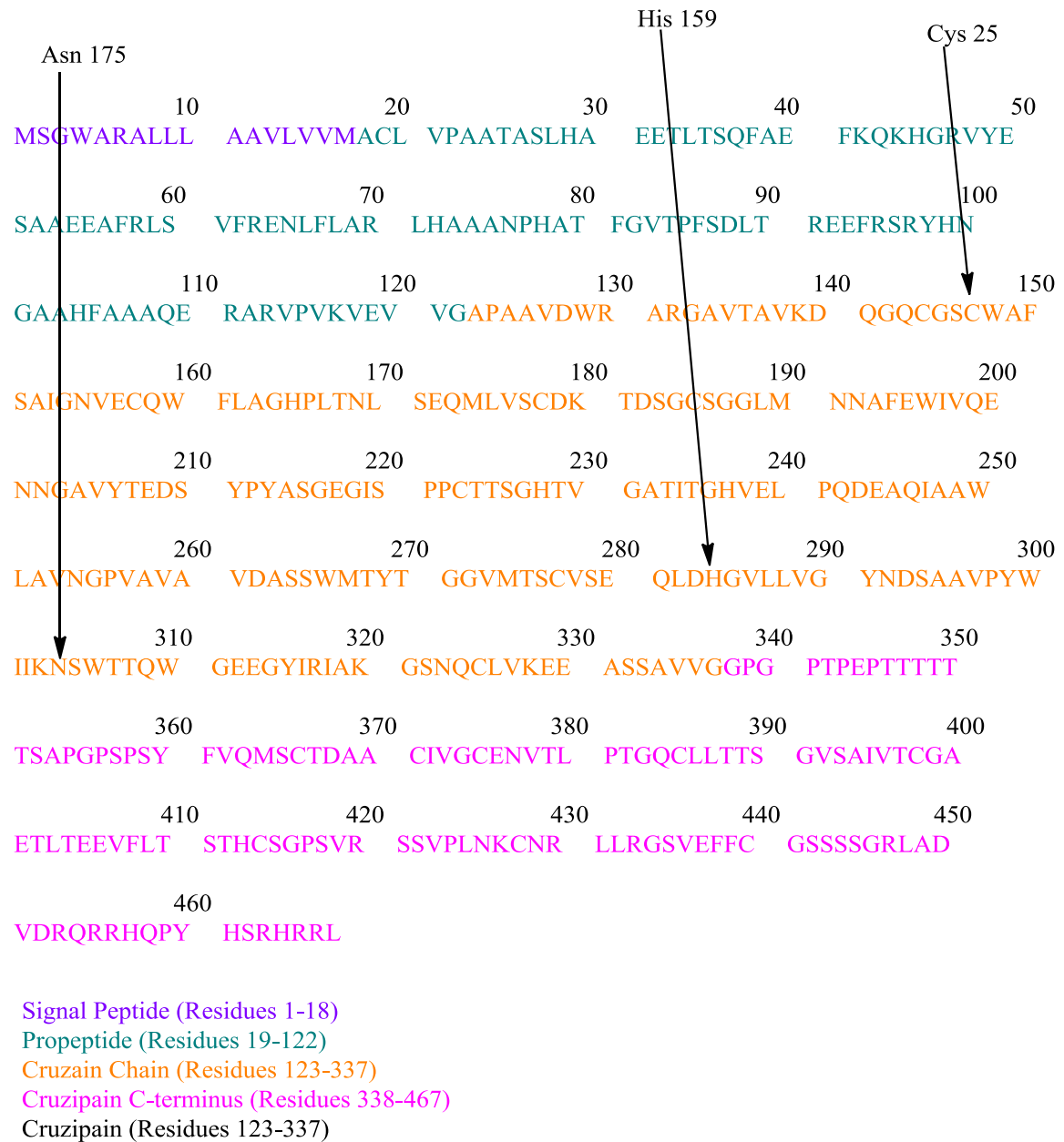
His 159

Cys 25

Asn 175

	10		20		30		40		50
MSGWARALLL		AAVLVVMACL		VPAATASLHA		EETLTSQFAE		FKQKHGRVYE	

	60		70		80		90		100
SAAEEAFRLS		VFRENLFLAR		LHAAANPHAT		FGVTPFSDLT		REEFRSRYHN	

	110		120		130		140		150
GAAHFAAAQE		RARVPVKVEV		VGAPAAVDWR		ARGAVTAVKD		QGQCGSCWAF	

	160		170		180		190		200
SAIGNVECQW		FLAGHPLTNL		SEQMLVSCDK		TDSGCSGGLM		NNAFEWIVQE	

	210		220		230		240		250
NNGAVYTEDS		YPYASGEGIS		PPCTTSGHTV		GATITGHVEL		PQDEAQIAAW	

	260		270		280		290		300
LAVNGPVAVA		VDASSWMTYT		GGVMTSCVSE		QLDHGVLLVG		YNDSAAVPYW	

	310		320		330		340		350
IIKNSWTTQW		GEEGYIRIAK		GSNQCLVKEE		ASSAVVGGPG		PTPEPTTTTT	

	360		370		380		390		400
TSAPGPSPSY		FVQMSCTDAA		CIVGCENVTL		PTGQCLLTTS		GVSAIVTCGA	

	410		420		430		440		450
ETLTEEVFLT		STHCSGPSVR		SSVPLNKCNR		LLRGSVEFFC		GSSSSGRLAD	

	460	
VDRQRRHQPY		HSRHRRL

Signal Peptide (Residues 1-18)
Propeptide (Residues 19-122)
Cruzain Chain (Residues 123-337)
Cruzipain C-terminus (Residues 338-467)
Cruzipain (Residues 123-337)

Figure 29. Amino acid residues of cruzipain. Acitve site residues are numbered using mature cruzain numbering(Taken and adapted from http://www.uniprot.org/uniprot/P25779)[76]
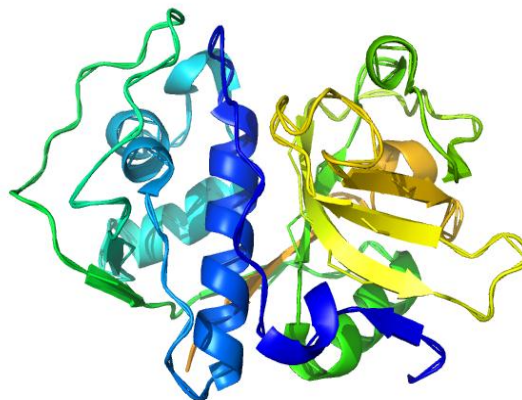
Figure 30. Crystal structure of the recombinant form of cruzipain, cruzain (PDB. 1ME3)[77]

Statement of purpose

In a collaborative project between the Trawick Biochemistry Group and Pinney Organic Sythesis Group, a library of small molecules containing a thiosemicarbazone moiety were synthesized and tested as potential therapeutic drugs for Chagas' disease through the inhibition of cruzain, a recombinant form of cruzipain. In a previous study by Siles *et al.*, a number of thiosemicarbazones were found to potent inhibitors of cruzain, exhibiting IC_{50} values in the lower nano-molar range.[78] Likewise, a previous study was conducted testing thiosemicarbazone compounds that were effective against cathepsin L and resulted in the discovery of a number of potent inhibitors of cruzain in the lower nano-molar range.[56]

In this study, a library of novel small compounds containing a thiosemicarbazones was tested to determine the inhibitory activity against cruzain. The compounds were tested using a fluorometric microplate assay. Results from this study provide more promising inhibitors for drug desing for the treatment of Chagas' disease.

61

CHAPTER FIVE

Experimental Procedure for the Evaluation of Potential Inhibitors of Cruzain for the Treatment of Chagas' Disease

The data for the current research were collected from a series of research and experiments performed as a collaborative research between the Trawick (biochemistry) and Pinney (organic synthesis) Laboratories in the Department of Chemistry and Biochemistry at Baylor University.

General Selection for Chemical Sources and Materials

The protein plasmid (Cruzain 72 18981562 V.HYNEK, Molecular Weight: 6,268.1) used for this experiment were provided by Dr. James McKerrow and Elizabeth Hansell from UCSF. The recombinant cruzain was subsequently purified with electrophoresis and visualized by SDS-PAGE by Dr. Wara Milenka Arispe Angulo at Baylor Univeristy.

The chemicals used for the enzyme assay are as follows. EDTA, disodium salt, dehydrate was purchased from Omni Pur (lot # 3577B034, Formula Weight: 372.24). The 30% Brij 35 solution was purchased from Sigma (Cas # 9002-92-0). The 99.9% dimethyl sulfoxide (DMSO) was purchased from Acros Organics (Lot # A0292589, Molecular Weight: 78.13). The substrate, benzyloxycarbonyl-phenylalanyl-arginyl-aminomethylcoumarin (Z-FR-AMC HCl) was purchased from BACHEM (Lot#1013575, Molecular Weight: 649.15). The DTT used was purchased from Omni Pur (Cas # 27565-41-9, Formula Weight: 154.25).

The instruments used are as follows. A Thermo Fluoroskan Ascent FL microplate reader and black 96 well Corning 3686 microplates were used to perform the assay. Graphpad 5.0 software was used to analyze data and used to perform non-linear regression analysis on data. The micropiptters and disposable tips were purchased from Eppendorf. The balance used to weigh various compounds and chemicals was a Mettler Toledo AX microbalance with an accuracy of 0.01 mg.

Preparation of 130 mM NaOAc buffer, pH 5.5

To prepare approximately 1 L of 130 mM NaOAc buffer, approximately 9.053 grams of sodium acetate (Molecular Weight: 82.03) into a 1 L volumetric flask. Approximately 1.125 mL of glacial acetic acid was added to adjust the pH. Ultrapure water was then carefully added to the volumetric flask and filled carefully to the marker as a magnetic spin bar was used to mix solution. The pH was checked and adjusted each time before running each experiment, using NaOH or glacial acetic acid.

Preparation of 80 mM DTT

The 80mM DTT (Molecular Weight: 154.25) was made fresh before each experiment. DTT was weighed using an analytical balance in a 12.34 μL to 1 mL ratio of DTT to 130 mM NaOAc buffer, pH 5.5. The mixture was then vortexed until completely dissolved to homogeneity. The solution was kept on ice until used.

Preparation of 40 mM EDTA

EDTA disodium salt (Molecular Weight: 372.2) was weighed on an analytical balance and added in a ratio of 1 mL of ultrapure water for every 14.89 mg of EDTA. The mixture was thoroughly vortexed and placed on ice until used.

Preparation of Assay Buffer

Assay buffer was made according to Table 11.

Table11. Preparation of Assay Buffer

Number of Columns	40 mM EDTA (µL)	80 mM DTT (µL)	30 mM Brij 35 (µL)	130 mM NaOAc (µL)
1	39	48.8	0.40	1200
2	78	97.5	0.80	2400
3	117	146.3	1.20	3600
4	156	195.0	1.60	4800
5	195	243.8	2.00	6000
6	234	292.5	2.40	7200
7	273	341.3	2.80	8400
8	312	390.0	3.20	9600
9	351	438.8	3.60	10800
10	390	487.5	4.00	12000
11	429	536.3	4.40	13200
12	468	585.0	4.80	14400

Preparation of Inhibitor

The 10 compounds tested in this study were synthesized by the Pinney research group at Baylor University. The 20 mM stock solutions were prepared by weighing out the dry compound and diluting it with 100% DMSO. The mixture was thoroughly vortexed and 1 to 10 serial dilutions were made from each stock solution. The inhibitors concentrations used for the enzyme assay were then prepared using Table 12.

Table 12. Preparation of Inhibitor Solutions

Final Concentration (nM)	Amount of Stock used (μL)	Stock Concentration (μM)	100% DMSO (μL)	Ultrapure Water (μL)
10000	10	2000	25	65
1000	10	200	25	65
100	10	20	25	65
50	5	20	30	65
10	10	2	25	65
1	10	0.2	25	65
0.1	10	0.02	25	65
0	0	---	35	65

Preparation of Enzyme Solution

Stock enzyme was stored at -80°C and aliquoted into smaller tubes. The enzyme aliquots were allowed to thaw on ice. Enzyme solution was prepared according to Table 13. The enzyme solution was then placed on ice until used in the assay.

Preparation of Substrate Solution

Substrate was prepared according to Table 14. The 30 mM stock solution was prepared by weighing out Z-FR-AMC using the analytical balance and diluting it with the proper amount of 100% DMSO. Because substrate is photo sensitive, foil was used to cover sample containers.

Table13. Preparation of Enzyme Solution

Number of Columns	40 mM EDTA (µL)	80 mM DTT (µL)	30 mM Brij 35 (µL)	130 mM NaOAc (µL)	Ultrapure water (µL)	Cruzain (µL)
2	42	52.5	0.56	1292.3	292.2	0.43
4	84	105.0	1.12	2584.6	584.4	0.87
8	168	210.0	2.24	5169.2	1168.8	1.73
12	252	315.0	3.36	7753.9	1753.2	2.60

Table 14. Preparation of Substrate Solution

Columns	Stock (30 mM)	100% DMSO (µL)	Ultrapure water (µL)
6	7.2	28.8	1404
7	8.4	33.6	1638
8	9.6	38.4	1872
9	10.8	43.2	2106
10	12.0	48.0	2340
11	13.2	52.8	2574
12	14.4	57.6	2808

Cruzain Assay

Once the solutions were prepared, the cruzain assay was done as follows. 100 µL of assay buffer was pipetted into the 96 microplate wells. Afterwards, 10 µL of inhibitor solution was added. Next 70 µL of enzyme solution was added and the microplate was placed in the microplate reader and shook for 10 seconds and incubated at 25°C in the

microplate reader. After the five minute incubation, 20 μL of substrate was added to each well and shook for 10 seconds and the fluorometric assay was run at and excitation and emission wavelength of 335 and 460 nm respectively at the final concentrations listed in Table 15. Data was analyzed using Graphpad 5.0.

Table 15. Final Concentrations in Cruzain Assay

EDTA (mM)	DTT (mM)	Brij (%)	NaOAc Buffer (mM)	DMSO (%)	Cruzain (nM)	Z-FR-AMC (μM)
1.0	2.5	0.01	100	2	0.1001	15.0

CHAPTER SIX

Results and Discussion for the Evaluation of Potential Inhibitors of Cruzain for the
Treatment of Chagas' Disease

Inhibition Studies with Thiosemicarbazones

This study was a collaborative project between Dr. Trawick's and Dr. Pinney's
research laboratory, which were responsible for the design, synthesis, and evaluation of
TSC derivatives as inhibitors of the cysteine protease cruzain for the treatment of
Chagas' disease. The fluorometric assay was run as stated in chapter five.

The release of fluorescent AMC from the cleavage of Z-RF-AMC was used as a
measure of enzyme activity (Figure 31).
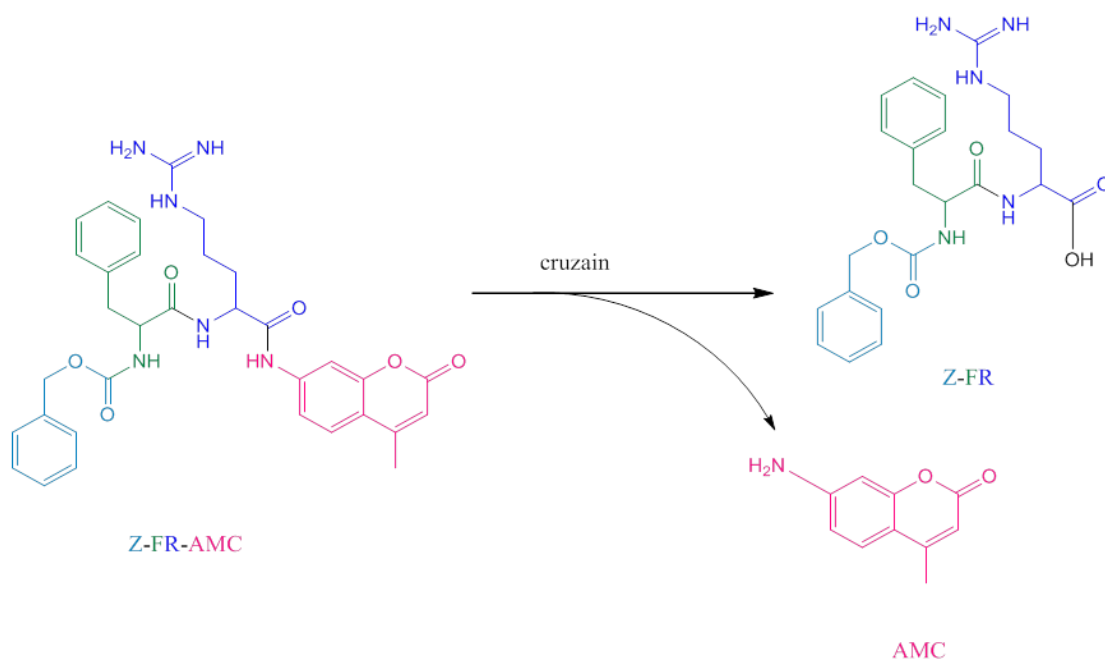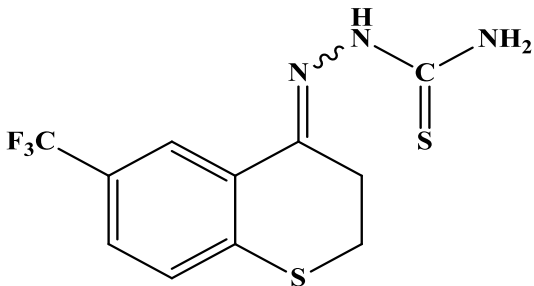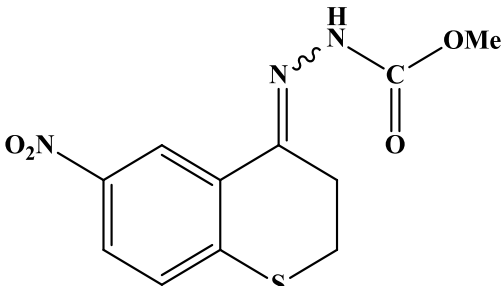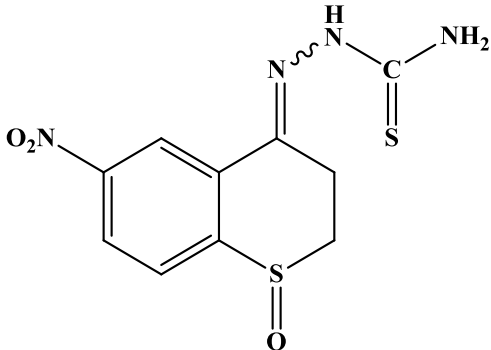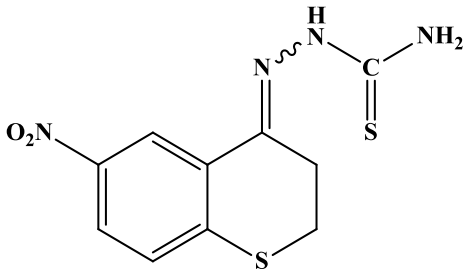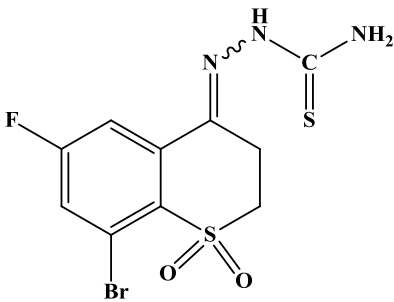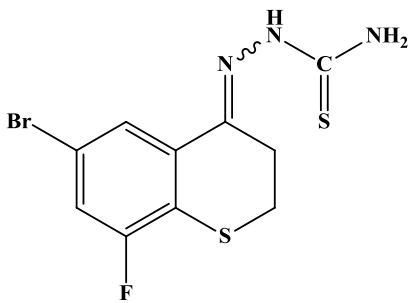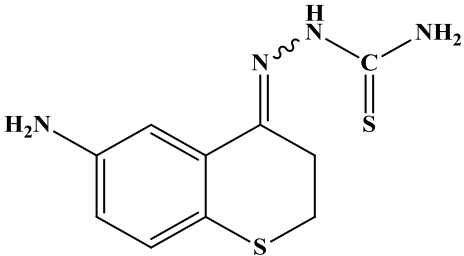
Figure 31. Hydrolysis of Z-FR-AMC substrate used as measure of cruzain activity
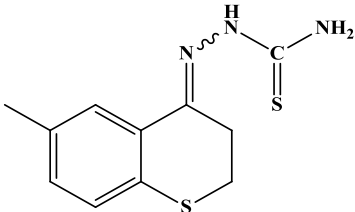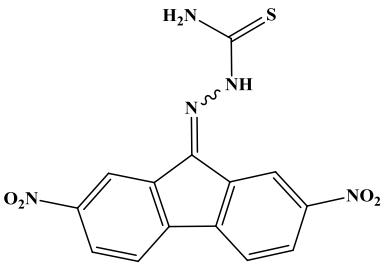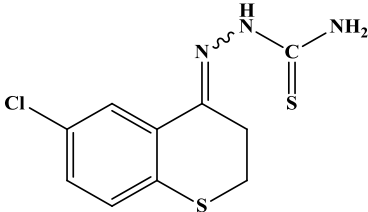
Data were analyzed by Graphpad and IC_{50} values were determined. IC_{50} values
correspond to the concentration of compound required for inhibition by 50% of the

enzyme's activity, and are used to measure the effectiveness of an inhibitor. Table 16

shows the ten inhibitor structures and their corresponding IC_{50} values.

Table 16. IC50 values of TSC Inhibitors against Cruzain

Compound	Structure	IC_{50} (nM) ± Standard Deviation
14		12.6 ± 0.34
15		>10,000
16		598.3 ± 53.09

Compound	Structure	IC_{50} (nM) ± Standard Deviation
17		84.7 ± 8.63
18		>10,000
19		10.25 ± 1.438
20		>10,000

Compound	Structure	IC$_{50}$ (nM) ± Standard Deviation
21		242.4 ± 36.14
22		>10,000
23		23.75 ± 2.23

Discussion of Thiosemicarbazone as Inhibitors of Cruzain

Figure 32 shows the general mode of action of cysteine proteases. Thiosemicarbazones are hypothesized to interact with the cysteine-25 residue in the active site of the cruzain. The exact mechanism of inhibition is unknown and further studies need to be conducted to determine the exact end product of the reaction between TSC and cruzain.

Out of the ten compounds tested, four possessed IC$_{50}$ values greater than 10,000 nM. Six of the ten compounds tested showed IC$_{50}$ values of less than 1000 nM. Out of those six compounds, three compounds, compounds **14**, **19**, and **23**, show IC$_{50}$ values of less than 50 nM.
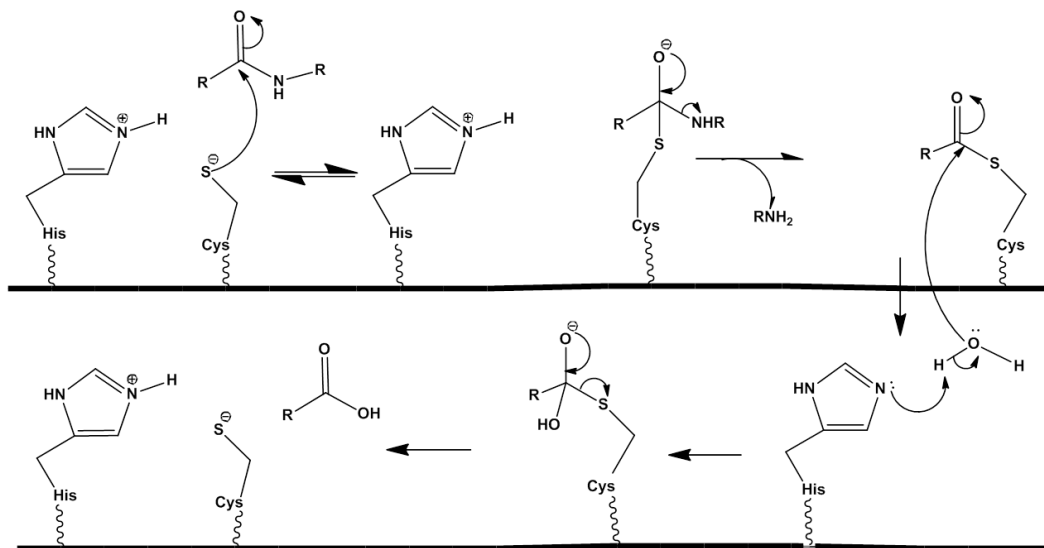
Figure 32. General mechanism of action of cysteine proteases such as cruzain

. Figure 34-36 show the inhibition of cruzain assay of compounds **14**, **19**, and **23** respectively. Figures 37-39 show the IC$_{50}$ curves of compounds **14**, **19**, and **23** respectively.
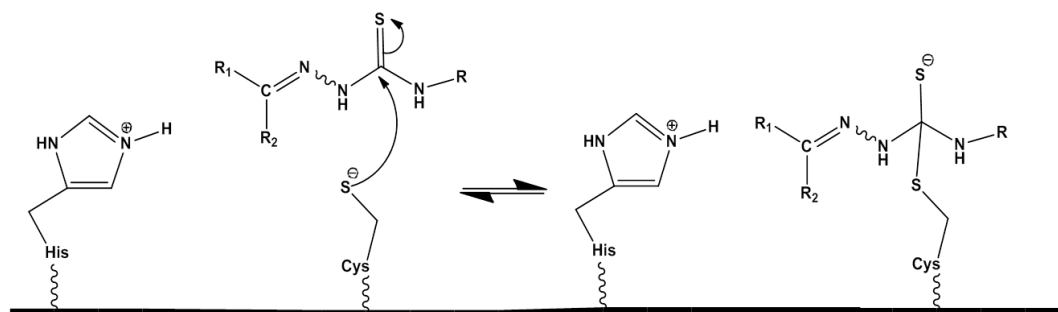
Figure 33. Hypothesized mechanism of action of thiosemicarbazone containing compound on cruzain active site
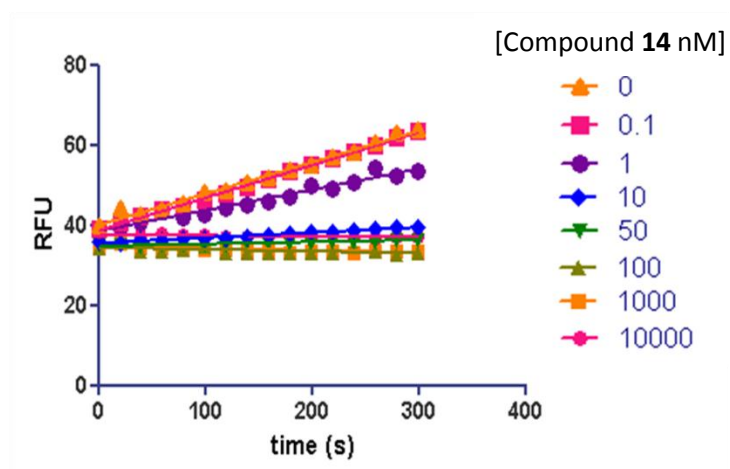
Figure 34. Inhibition of cruzain assay by compound **14**
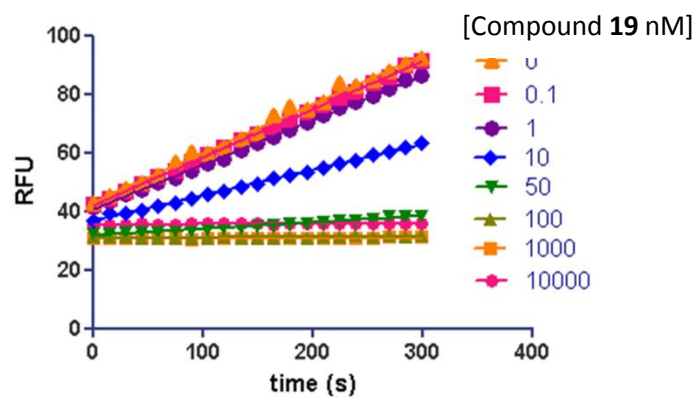
Figure 35. Inhibition of cruzain assay by compound **19**
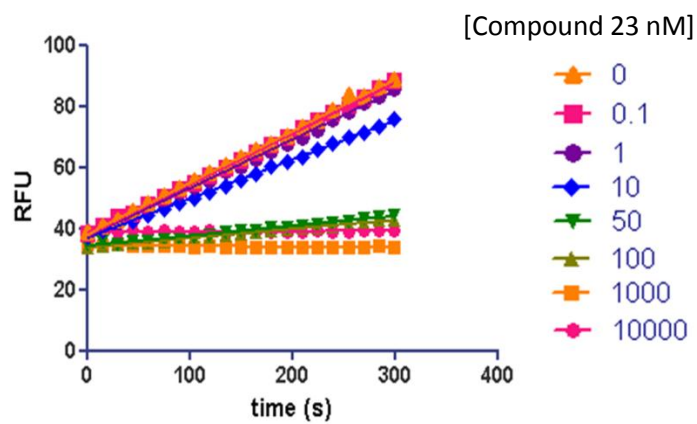
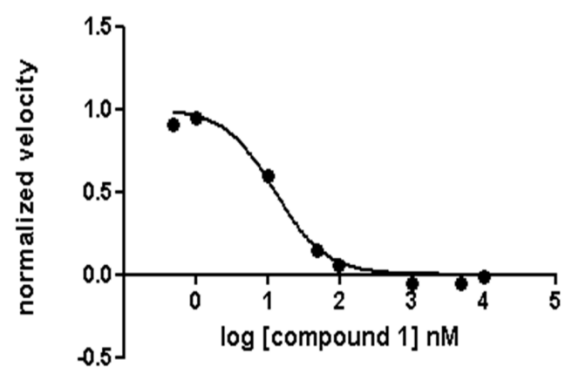Figure 36. Inhibition of cruzain assay by compound **23**
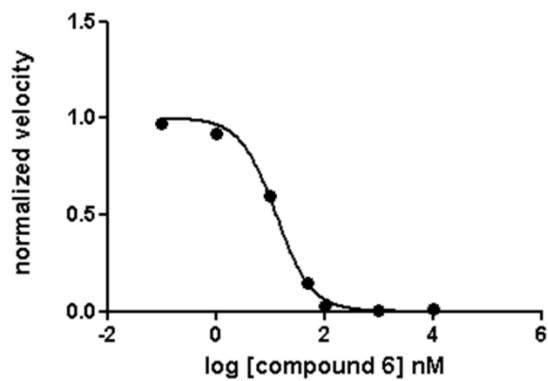
Figure 37. IC$_{50}$ curve of compound **14**

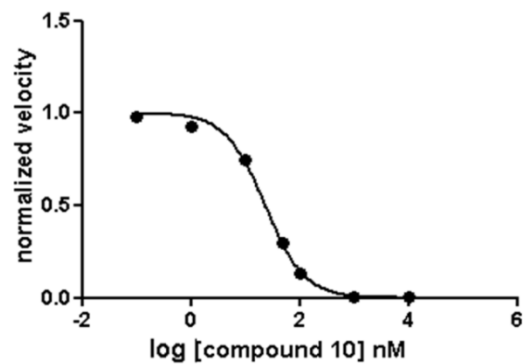
Figure 38. IC$_{50}$ curve of compound **19**

Figure 39. IC$_{50}$ curve of compound **23**

Future Studies

This study further confirms that thiosemicarbazones are effective inhibitors of cruzain *in vitro,* suggesting their potential role as therapeutic drugs for the treatment of Chagas' disease. Three compounds showed very good inhibition ($IC_{50} \leq 30nM$) of cruzain. Further testing such as advanced kinetics test to determine the mechanism of inhibition need to be performed in future studies. Overall, the experiment shows promising results for the discovery of a new anti-trypanasomal drug that exhibits low toxicity levels.

APPENDICES

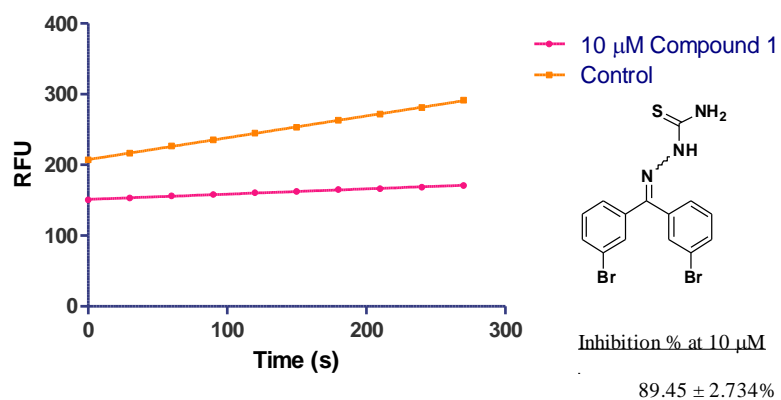Determination of Inhibitory Activity of TSC against Cathepsin B

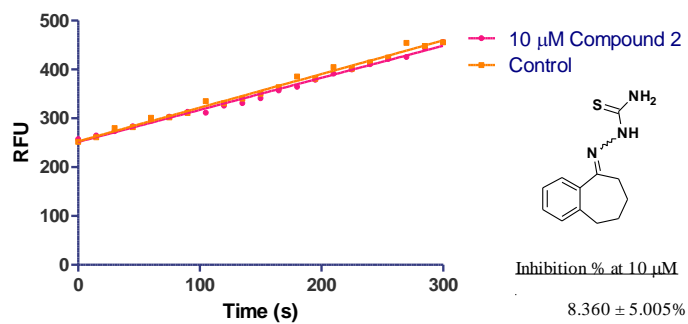Figure A1. Determination of inhibitory activity of compound **1**

Figure A2. Determination of inhibitory activity of compound **2**
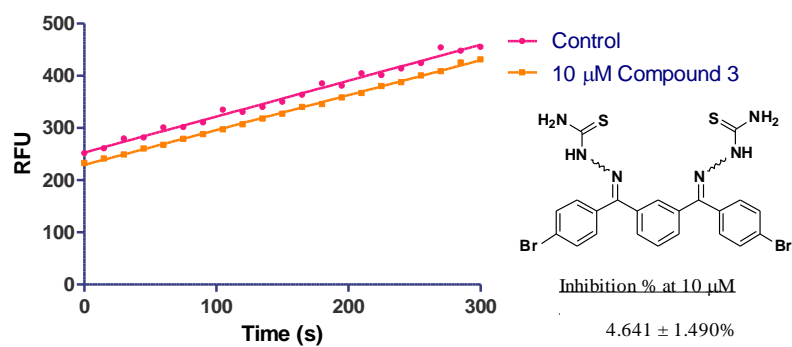
Figure A3. Determination of inhibitory activity of compound **3**

Figure A4. Determination of inhibitory activity of compound **4**

Figure A5. Determination of inhibitory activity of compound **5**

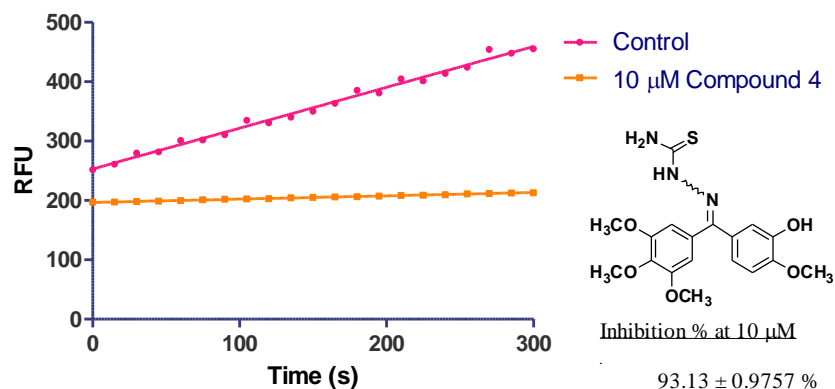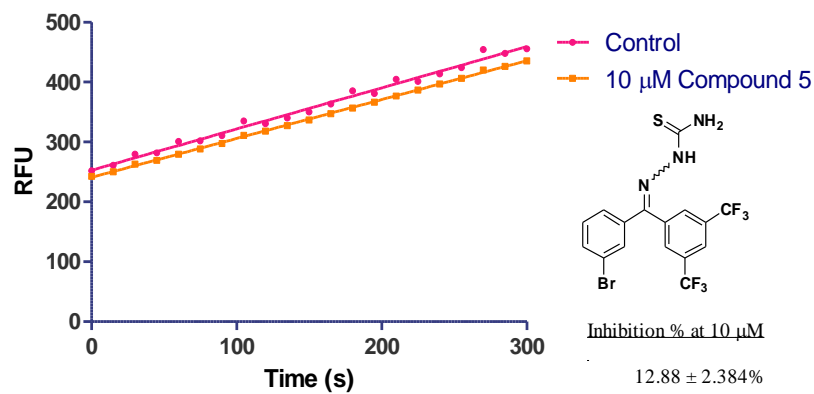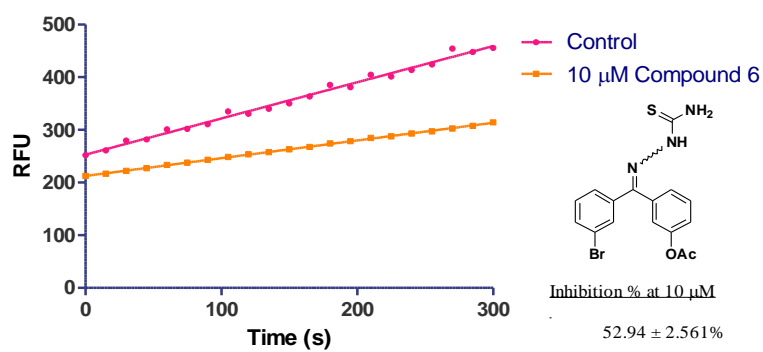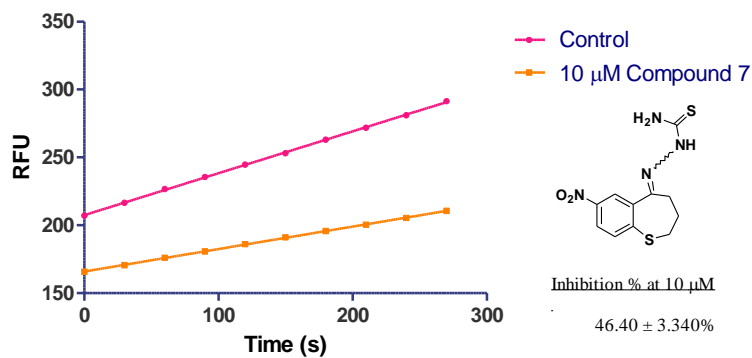Figure A6. Determination of inhibitory activity of compound **6**

Figure A7. Determination of inhibitory activity of compound **7**

Figure A8. Determination of inhibitory activity of compound **8**

Figure A9. Determination of inhibitory activity of compound **9**

Figure A10. Determination of inhibitory activity of compound **10**

Figure A11. Determination of inhibitory activity of compound **11**

Figure A12. Determination of inhibitory activity of compound **12**

Figure A13. Determination of inhibitory activity of compound **13**

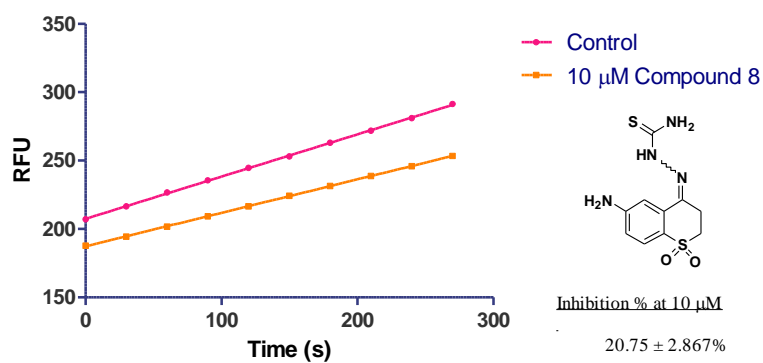Determination of Ihnibitory Activity of TSC against Cruzain

Figure B1. Determination of inhibitory activity of compound **14**

Figure B2. Determination of inhibitory activity of compound **15**

Figure B3. Determination of inhibitory activity of compound **16**

Figure B4. Determination of inhibitory activity of compound **17**

Figure B5. Determination of inhibitory activity of compound **18**
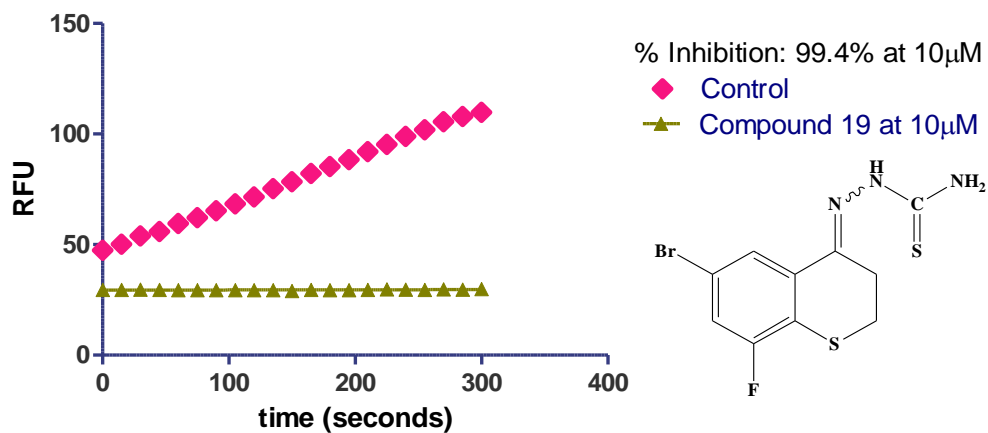
Figure B6. Determination of inhibitory activity of compound **19**
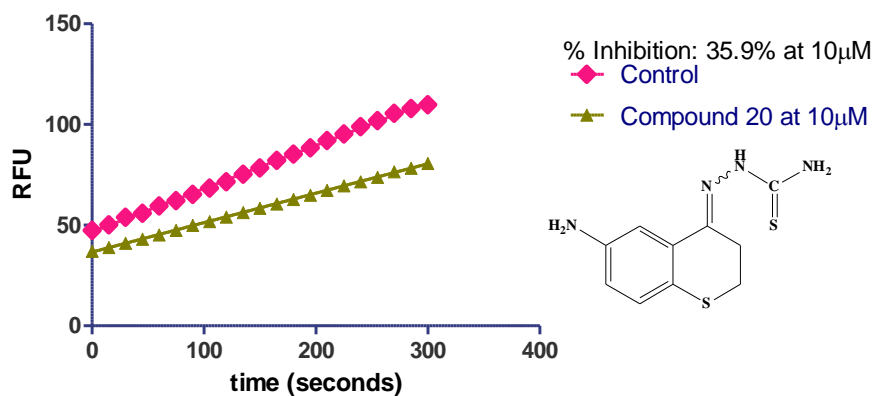
Figure B7. Determination of inhibitory activity of compound **20**

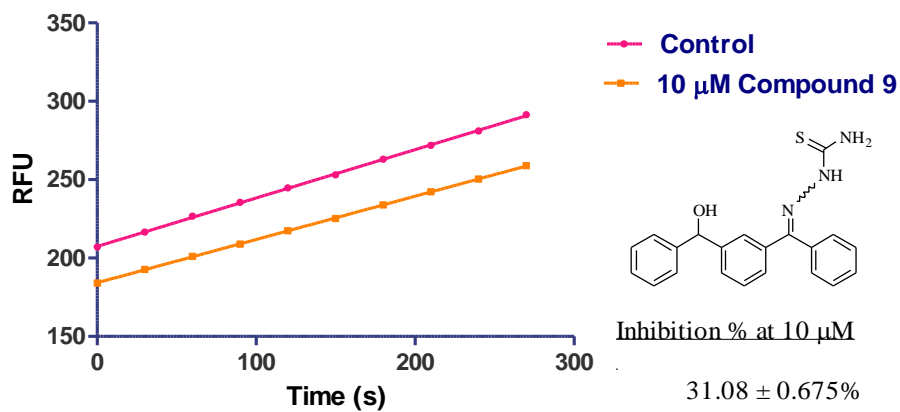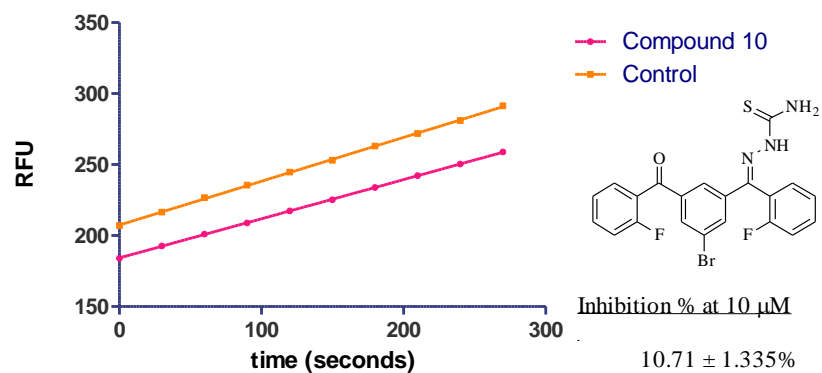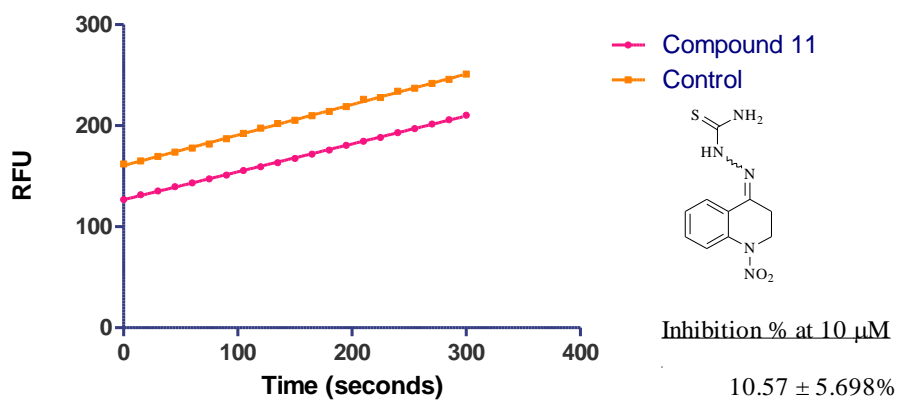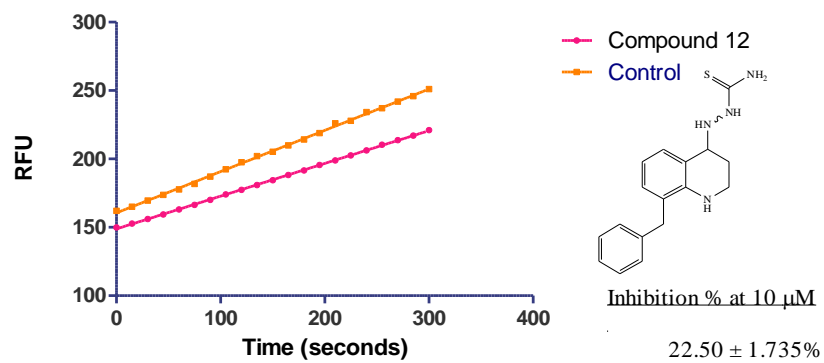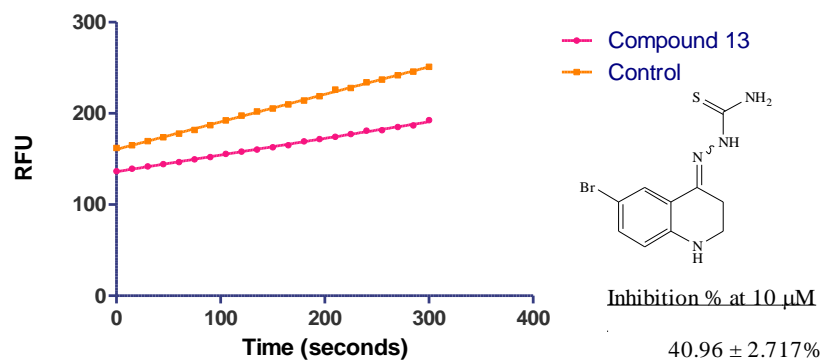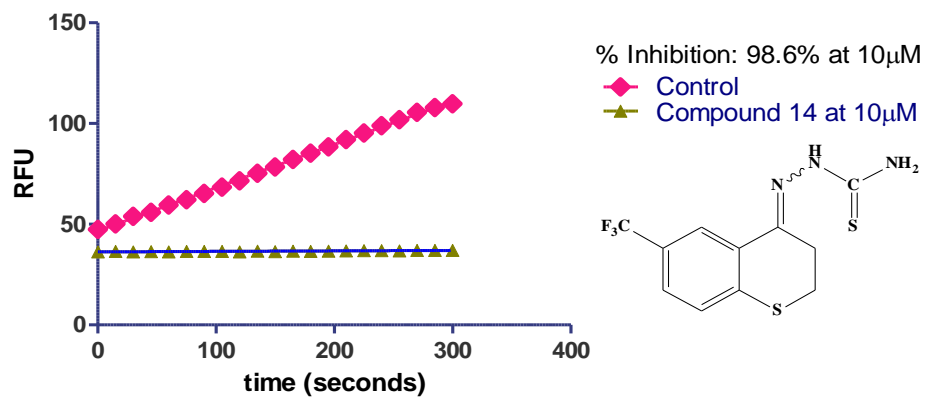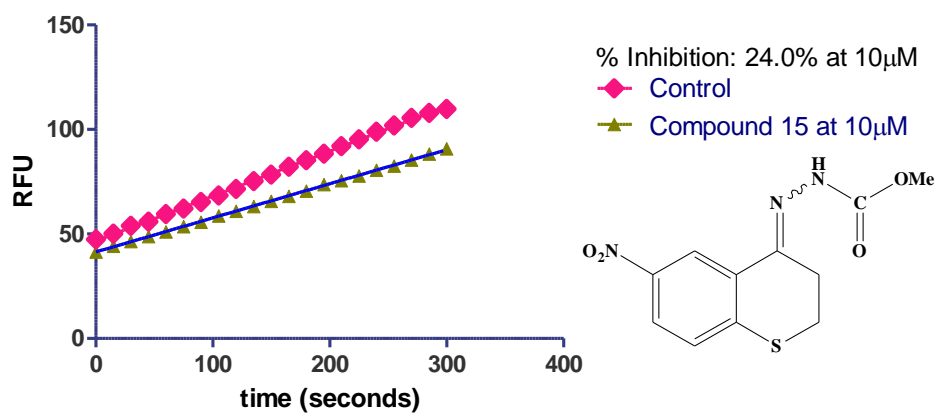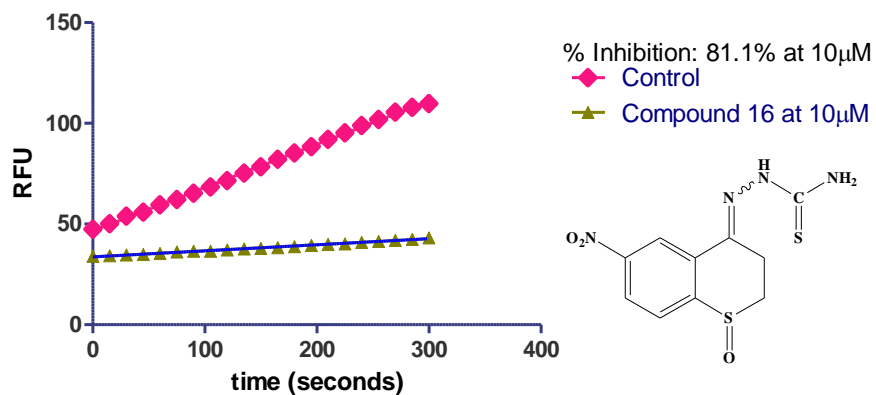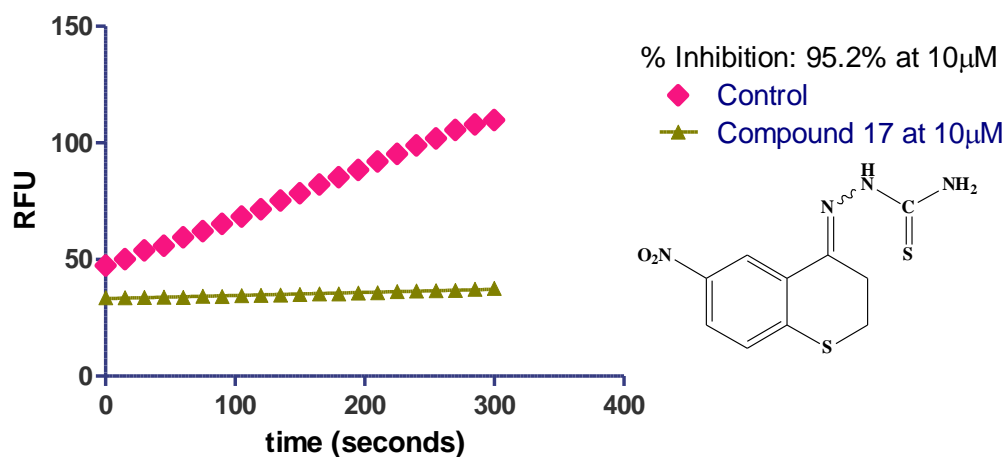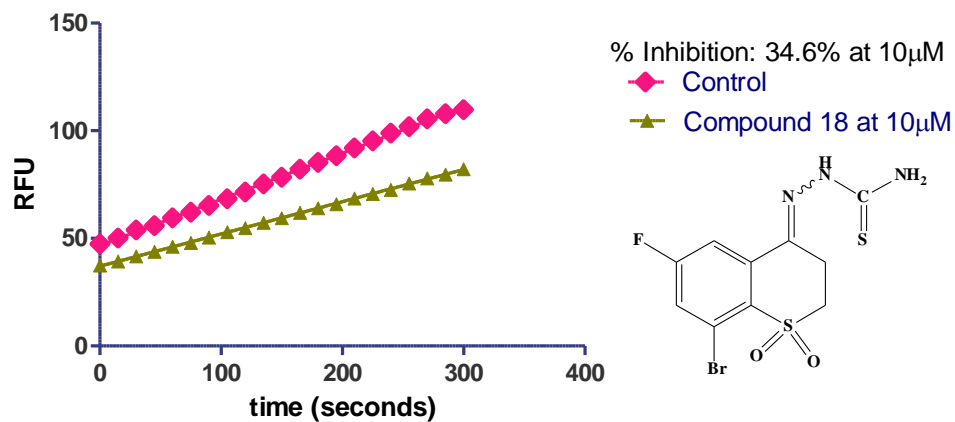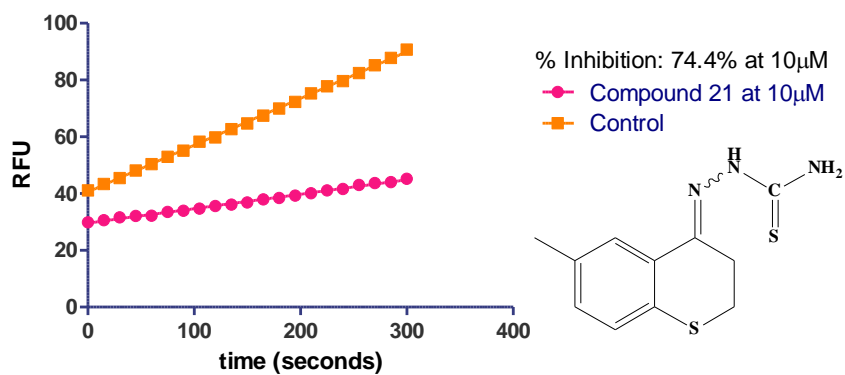Figure B8. Determination of inhibitory activity of compound **21**

% Inhibition: 19.2% at 10μM
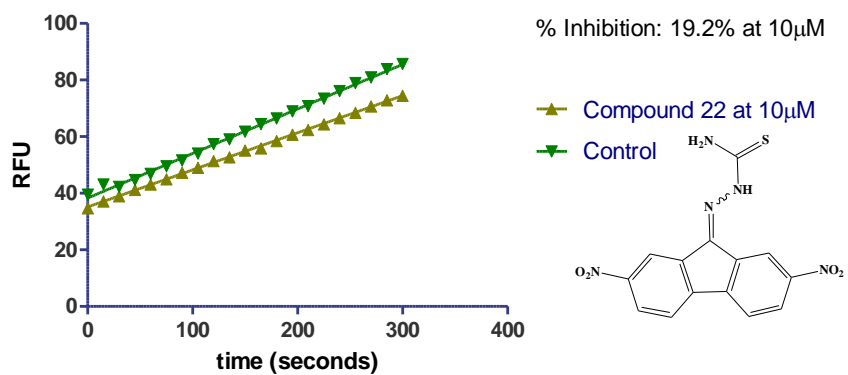
Figure B9. Determination of inhibitory activity of compound **22**

% Inhibition: 97.8% at 10μM
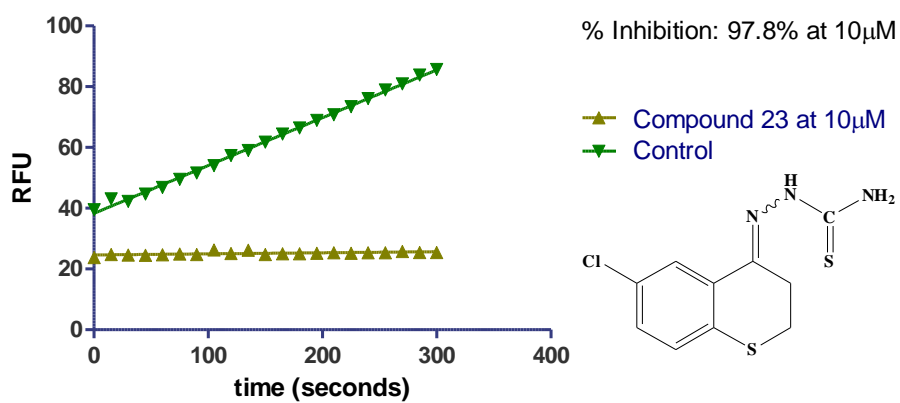
Figure B10. Determination of inhibitory activity of compound **23**

APPENDIX C

Determination of IC$_{50}$ for TSC against Cruzain

Sigmoidal dose-response (variable slope)	
Best-fit values	
Bottom	= 0.0
Top	= 1.000
LogEC50	1.083
HillSlope	-1.578
EC50	12.11
Std. Error	
LogEC50	0.04607
HillSlope	0.2776
95% Confidence Intervals	
LogEC50	0.9702 to 1.196
HillSlope	-2.257 to -0.8986
EC50	9.338 to 15.69
Goodness of Fit	
Degrees of Freedom	6
R square	0.9922
Absolute Sum of Squares	0.01157
Sy.x	0.04391
Constraints	
Bottom	Bottom = 0.0
Top	Top = 1.000
Number of points	
Analyzed	8
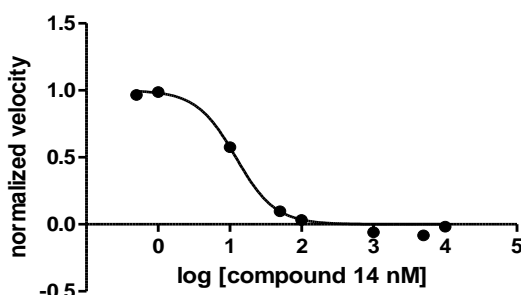
Figure C1. Determination of IC$_{50}$ for compound **14**

Sigmoidal dose-response (variable slope)	
Best-fit values	
Bottom	= 0.0
Top	= 1.000
LogEC50	2.754
HillSlope	-0.9775
EC50	567.5
Std. Error	
LogEC50	0.08294
HillSlope	0.1325
95% Confidence Intervals	
LogEC50	2.551 to 2.957
HillSlope	-1.302 to -0.6534
EC50	355.6 to 905.5
Goodness of Fit	
Degrees of Freedom	6
R square	0.9844
Absolute Sum of Squares	0.01847
Sy.x	0.05548
Constraints	
Bottom	Bottom = 0.0
Top	Top = 1.000
Number of points	
Analyzed	8
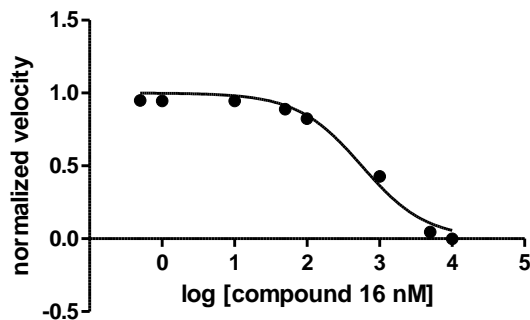
Figure C2. Determination of IC$_{50}$ for compound **16**

Sigmoidal dose-response (variable slope)	
Best-fit values	
Bottom	= 0.0
Top	= 1.000
LogEC50	1.476
HillSlope	-0.9207
EC50	29.96
Std. Error	
LogEC50	0.06850
HillSlope	0.1371
95% Confidence Intervals	
LogEC50	1.300 to 1.653
HillSlope	-1.273 to -0.5681
EC50	19.97 to 44.94
Goodness of Fit	
Degrees of Freedom	5
R square	0.9870
Absolute Sum of Squares	0.01337
Sy.x	0.05171
Constraints	
Bottom	Bottom = 0.0
Top	Top = 1.000
Number of points	
Analyzed	7
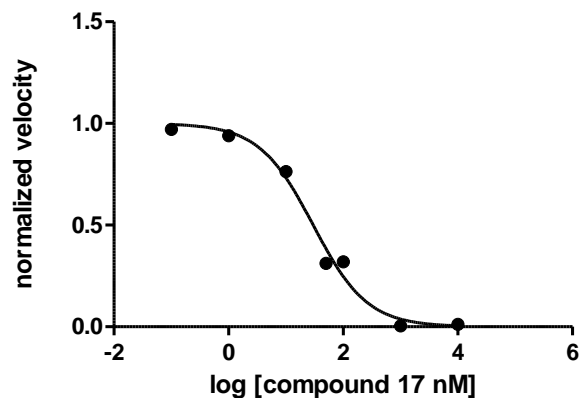
Figure C3. Determination of IC_{50} for compound **17**

Sigmoidal dose-response (variable slope)	
Best-fit values	
Bottom	= 0.0
Top	= 1.000
LogEC50	1.011
HillSlope	-1.100
EC50	10.26
Std. Error	
LogEC50	0.04357
HillSlope	0.1083
95% Confidence Intervals	
LogEC50	0.8990 to 1.123
HillSlope	-1.379 to -0.8217
EC50	7.925 to 13.27
Goodness of Fit	
Degrees of Freedom	5
R square	0.9953
Absolute Sum of Squares	0.004949
Sy.x	0.03146
Constraints	
Bottom	Bottom = 0.0
Top	Top = 1.000
Number of points	
Analyzed	7
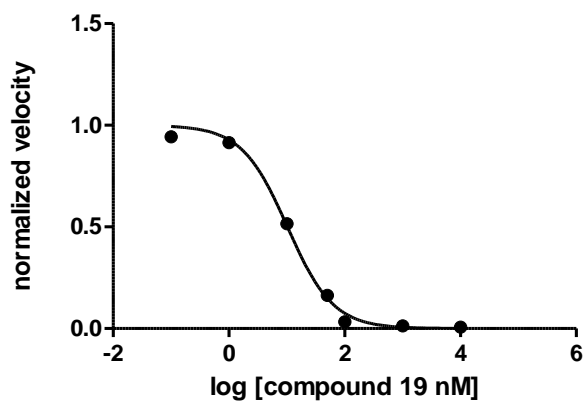
Figure C4. Determination of IC_{50} for compound **19**

Sigmoidal dose-response (variable slope)	
Best-fit values	
Bottom	= 0.0
Top	= 1.000
LogEC50	2.339
HillSlope	-1.403
EC50	218.4
Std. Error	
LogEC50	0.03875
HillSlope	0.1138
95% Confidence Intervals	
LogEC50	2.240 to 2.439
HillSlope	-1.695 to -1.110
EC50	173.7 to 274.8
Goodness of Fit	
Degrees of Freedom	5
R square	0.9969
Absolute Sum of Squares	0.003253
Sy.x	0.02551
Constraints	
Bottom	Bottom = 0.0
Top	Top = 1.000
Number of points	
Analyzed	7
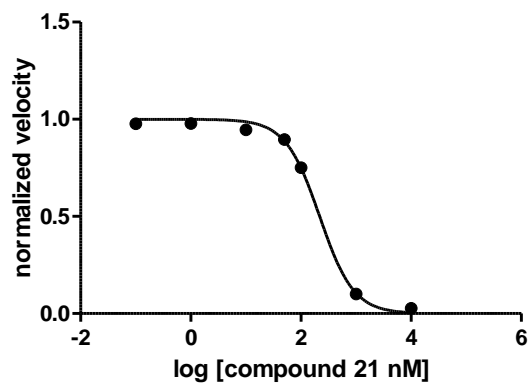
Figure C5. Determination of IC_{50} for compound **21**

| Sigmoidal dose-response (variable slope)	
Best-fit values	
Bottom	= 0.0
Top	= 1.000
LogEC50	1.408
HillSlope	-0.9411
EC50	25.58
Std. Error	
LogEC50	0.05097
HillSlope	0.1021
95% Confidence Intervals	
LogEC50	1.277 to 1.539
HillSlope	-1.203 to -0.6786
EC50	18.91 to 34.59
Goodness of Fit	
Degrees of Freedom	5
R square	0.9930
Absolute Sum of Squares	0.007286
Sy.x	0.03817
Constraints	
Bottom	Bottom = 0.0
Top	Top = 1.000
Number of points	
Analyzed	7
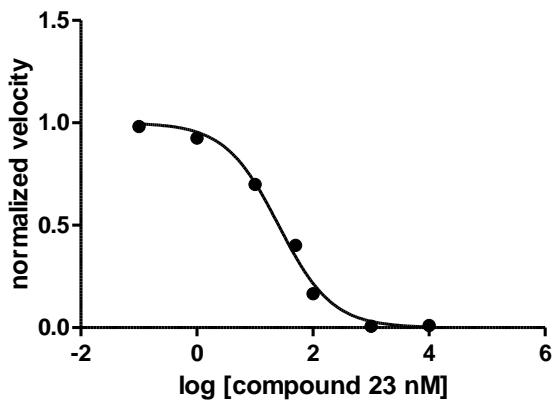
Figure C6. Determination of IC_{50} for compound **23**

REFERENCES:

[1] "What is Cancer?" National Cancer Institute. *Comprehensive Cancer Information – National Cancer Institute.* <http://www.cancer.gov>

[2] "Cancer Genetic Overview" National Cancer Institute. *Comprehensive Cancer Information – National Cancer Institute.* <http://www.cancer.gov>

[3] "Test and Diagnosis" *Cancer.* <http://www.mayoclinic.com>

[4] "Cancer Prevelance: How many people have cancer?" *American Cancer Society.* <www.cancer.org>

[5] "Symptoms" *Cancer.* <http://www.mayoclinic.com>

[7] "Types of Treatment." National Cancer Institute. *Comprehensive Cancer Information – National Cancer Institute.* <http://www.cancer.gov>

[8] "Chemotherapy Side Effects Fact Sheets" National Cancer Institute. *Comprehensive Cancer Information – National Cancer Institute.* <http://www.cancer.gov>

[9] "Definition" *Cancer.* <http://www.mayoclinic.com>

[10] Boris Turk. *Targeting proteases: success, failures, and future prospects.* Nature Review Drug Discovery. 2006

[11] Benelita Tina Elie, Vasilena Gocheva, Tanaya Shree, Stacie A. Dalrymple, Leslie J. Holsinger, Johanna A. Joyce. *Identification and pre-clinical testing of a reversible cathepsin protease inhibitor reveals anti-tumor efficacy in pancreatic cancer model.* Biochimie 92 (2010) 1618-1624.

[12] L Mach, H Schwihla, K Stüwe, A D Rowan, J S Mort, and J Glössl. *Activation of procathepsin B in human hepatoma cells: the conversion into the mature enzyme relies on the action of cathepsin B itself.* Biochem J. (1993) 293, 437 – 442.

[13] L Mach, J S Mort and J Glössl. *Maturation of human procathepsin B. Proenzyme activation and proteolytic processing of the precursor to the mature proteinase, in vitro, are primarily unimolecular processes.* The Journal of Biological Chemistry. Vol. 269, No. 17, pp. 13030 – 13035. 1994.

[14] Vito Turk and Boris Turk. *Lysosomal Cysteine Proteases and Their Protein Inhibitors: Recent Developments.* Acta Chim. Slov. 2008, 55, 757 – 737.

[15] Jerica Rozman Pungercar, Dejan Caglic, Mohammed Sajid, Marko Dolinar, Olga Vasiljeva, Urska Pozgan, Duscan Turk, Matthew Bogyo, Vito Turk, and Boris Turk. *Autocatalytic processing of procathepsin B is triggered by proenzyme activity.* FEBS Journal 276. (2009). 660 – 668.

[16] PBD 2IPP, CP Huber, RL Campbell, S. Hasnain, T. Hirama, R. To. Crystal Structure of the tetragonal form of human liver cathepsin B. 2009.

[17] Vito Turk, Boris Turk, and Duscan Turk. *Lysosomal cysteine proteases: facts and opportunities.* The EMBO Journal. Vol. 20, No. 17, pp. 4629 – 4633. (2001).

[18] PDB 2PBH, D. Turk, M. Podobnik, R. Kuheli, M. Dolinar, V. Turk. Crystal Structures of human procathepsin B at 3.2 and 3.3 Angstroms resolution reveal an interaction motif between a papain like cysteine protease and its propeptide. FEBS Lett. 1996.

[20] Dora Cavallo-Medved, Kamiar Moin, Bonnie Sloane. *Cathepsin B.* UCSD Nature Molecule Pates. 2011

[21] Bonnie F. Sloane, Kamiar Moin, Evzen Krepela, and Jurij Rozhin. *Cathepsin B and its endogenous inhibitors: the role in tumor malignancy.* Cancer and Metastasis Reviews 9: 333 – 352, 1990.

[22] Atsushi Yamamoto, Koji Tomoo, Ken-ichi Matsugi, Tadaoki Hara, Yasuko In, Mitsuo Murata, Kunihiro Kitamura, and Toshimasa Ishida. *Structural basis for development of cathepsin B-specific noncovalent-type inhibitor: crystal structure of cathepsin B-E64c complex.* Biochimica et Biophysica Acta 1597 (2002) 244 – 251.

[23] D. Musil, D. Zucic, D. Truk, R.A. Engh, I. Mayr, R. Huber, T. Popovic, V. Turk, T. Towatari, N. Katunuma, and W. Bode. *The refined 2.15 Å X-ray crystal structure for human liver cathepsin B: the structural basis for specificity.* The EMBO Journal. Vol. 10, no.9, pp. 2321 – 2330, 1990.

[24] Jianxing Song, Ping Xu, Hui Xiang, Zhengding Su, Andrew C. Storer, and Feng Ni. *The active-site residue Cys-29 is responsible for the neutral-pH inactivation and refolding barrier of human cathepsin B.* FEBS Letters 475 (2000) 157 – 162.

[25] Boris Turk, Iztok Dolenc, Eva Zerovnik, Duscan Turk, Franc Gubensek, and Vito Turk. *Human Cathepsin B is a Metastable Enzyme Stabilized by Specific Ionic Interactions Associated with the Active Site.* Biochemistry 1994, 33, 14800 – 14806.

[26] The UniProt Consortium The Universal Protein Resource (UniProt) in 2010. *http://www.uniprot.org/uniprot/P07858.html* (accessed April 11, 2012).

[27] Protein Data Bank 1HUC. D. Musil, D. Zucic, D. Turk, RA Engh, I Mayr, R Huber, T Popovic, V Turk, T Towatari, N Katunuma, *et al.* The refined 2.15 A X-ray crystal structure of human liver cathepsin B: the structural basis for specificity. The EMBO Journal. Vol 10, no. 9, 2321-2330. 1991

[28] John S. Mort and David Buttle. *Molecules in Focus: Cathepsin B.* Int. J. Biochem. Cell Biol. Vol 29, No. 5, pp. 715 – 720, 1997.

[29] R. Frlan and S. Gobec. *Inhibitors of Cathepsin B.* Current Medicinal Chemistry, 2006, 13, 2309 – 2327.

[30] B.-Z. Zeng, X.-L. Pan, N.-H Tan, J. Xiong, Y.-M. Zhang. *Natural bioflavones as novel inhibitors of cathepsin B and K.* European Journal of Medicinal Chemistry 41 (2006) 1247 – 1252.

[31] Joanne C. Krupa, Sadiq Hasnain, Dorit K. Nagler, Robert Menard, and John S. Mort. *S'_2 substrate specificity and the role of His^{110} and His^{111} in the exopeptidase activity of human cathepsin B.* Biochem. J. (2002) 361, 613 – 619.

[32] Chantal Illy, Omar Quraishi, Jing Wang, Enrico Purisima, Thierry Vernet, and John S. Mort. *Role of the Occluding Loop in Cathepsin B Activity.* The Journal of Biological Chemistry, 1997, vol 272, no. 2, 1197-1202.

[33] Heidrun Kirschke, Peter Wikstrom, and Elliott Shaw. *Active center differences between cathepsin L and B: the S_1 binding region.* FEBS Journal, vol. 228, no.1, 128 – 130.

[34] Keita Matsumoto, Mitsuo Murata, Shigeyuki Sumiya, Kazutoshi Mizoue, Kunihiro Kitamura, and Toshimasa Ishida. *X-Ray crystal structure of papain complexed with cathepsin B-specific covalent-type inhibitor: substrate specificity and inhibitory activity.* Biochimica et Biophysica Acta 1383, (1998) 93 – 100.

[35] Atsushi Yamamoto, Koji Tomoo, Ken-ichi Matsugi, Tadaoki Hara, Yasuko In, Mitsuo Murata, Kunihiro Kitamura, and Toshimasa Ishida. *Structual basis for development of cathepsin B-specific noncovalent-type inhibitor: crystal structure of cathepsin B-E64c complex.* Biochimica et BIophysica Acta 1597 (2002) 244 – 251.

[36] Daiya Watanabe, Atsushi Yamamoto, Koji Tomoo, Keita Matsumoto, Mitsuo Murata, Kunihiro Kitamura, and Toshimasa Ishida. *Quantitative Evaluation of Each Catalytic Subsite of Cathepsin B for Inhibitory Activity Based on Inhibitory Activity – Binding Mode Relationship of Epoxysuccinyl Inhibitors by X-ray Crystal Structure Analyses of Complexes.* J. Mol. Biol. (2006) 362, 979 – 993.

[37]Vito Turk and Boris Turk. *Lysosomal Cysteine Proteases and Their Protein Inhibitors: Recent Developments.* Acta Chim. Slov. 2008, 55, 757 – 737.

[38] Jochen Reiser, Brian Adair, and Thomas Reinheckel. Specialized Roles for Cysteine Cathepsins in Health and Disease. The Journal of Clinical Investigation. Volume 120, Number 10, 2010.

[39] Hohan Sundelof, Johan Sundstrom, Oskar Hansson, Maria Eriksdotter-Jonhagen, Vilmantas Giedraitis, Anders Larsson, Malin Degerman-Gunnarsson, Martin Ingelsson, Lennart Minthon, Kaj Blennow, Lena Kilander, Hans Basun, and Lars Lannfelt. Higher Cathpsin B levels in Plasma in Alzheimer's Disease Compared to Healthy Controls. Journal of Alzheimer's Disease 22 (2010) 1223-1230.

[40] Vivian Hook, Gregory Hook, and Mark Kindy. Pharmacogenetic features of cathepsin B inhibitors that improve memory deficit and reduce amyloid-β related to Alzheimer's disease. Biol. Chem. Vol. 391, 861-872. 2010.

[41] Izabela Podgorski and Bonnie F. Sloane. Cathepsin B and its role(s) in cancer progression. Biochem. Soc. Symp. 70, 263 – 276. (2003)

[42] Paulo C. Slmeida, Iseli L. Nantes, Jair R. Chagas, Claudia C.A. Rizzit, Adelaide Faljoni-Alario, Euridice Carmona, Luiz Juliano, Helena B. Nadar, and Ivarne L. S. Tersariol. *Cathepsin B Activity Regulation: Heparin Like Glycosaminoglycans protect*

[43] Shiquing Yan and Bonnie Sloane. Molecular Regulation of Human Cathepsin B: Implications in Pathologies. Biol. Chem., Vol. 384, 845 – 854. (2003)

[44] Bonnie F. Sloane, Shiqing Yan, Izabela Podgorski, Bruce E. Linebaugh, Michael L. Cher, Jianxin Mai, Dora Cavallo-Medved, Mansoureh Sameni, Julie Dosescu, and Kamiar Moin. Cathepsin B and tumor proteolysis: contribution of the tumor microenvironment. Seminars in Cancer Biology 15 (2005) 149-157.

[45] Stefanie Roshy, Bonnie F. Sloane, and Kamiar Moin. Pericellular cathepsin B and malignant progression. Cancer and Metastasis Reviews 22: 271 – 286. (2003).

[46] Barbara Fingleton and Conor Lynch. Chapter 3: Cancer in Context: Importance of the Tumor Microenvironment. Cell-extracellular Matrix Interaction in Cancer 2010, 43-63.

[47] Paola Matarrese, Barbara Ascione, Laura Ciarlo, Rosa Vona, Carlo Leonetti, Marco Scarsella, Anna M. Mileo, Caterina Catricala, Marco G. Paggi, and Walter Malorni. Cathepsin B inhibition interferes with metastatic potential of human melanoma: an *in vitro* and *in vivo* study. Molecular Cancer 2010, 9:207.

[48] Bernadette C Victor, Arulselvi Anbalagan, Mona M Mohamed, Bonnie F Sloane, and Dora Cavallo-Medved. Inhibition of cathepsin B activity attenuates extracellular matrix degradation and inflammatory breast cancer invasion. Breast Cancer Research 2011.

[49] Jennifer E. Koblinski, Mamoun Abram, Bonnie F. Sloane. Unraveling the roles of proteases in cancer. Clinica Chimica Acta 291, 113-135 (2000).

[50] Boris Turk. *Targeting proteases: successes, failures, and future prospects.* Nature Reviews Drug Discovery **5**, 785-799 (September 2006)

[51] R. Frlan and S. Gobec. Inhibitors of Cathepsin B. Current Medicinal Chemistry, 2006, 13, 2309-2327.

[52] Amir Masoud Sadaghiani, Steven H.L. Verhelst, Vasilena Gocheva, Kimberly Hill, Eva Majerova, Sherman Stinson, Johanna A. Joyce, and Matthew Bogyo. Design, synthesis, and evaluation of *in vivo* potency and selectivity of epoxysuccinyl-based inhibitors of papain family cysteine proteases. Chemistry and Biology 14, 499-511. (2007)

[53] Atsushi Yamamoto, Koji Tomoo, Ken-ichi Matsugi, Tadaoki Hara, Yasuko In, Mitsuo Murata, Kunihiro Kitamura, Toshimasa Ishida. Structural basis for development of cathepsin B-specific noncovalent –type inhibitor: crystal structure of cathepsin B-E64c complex. Biochimica et Biophysica Acta 1597 (2002) 244-251.

[54] T Schirmeister and U. Kaeppler. Non-Peptidic Inhibitors of Cysteine Proteases. Mini Reviews in Medicinal Chemistry, 2003, 3, 361-373.

[55] Doron C. Greenbaum, Zachary Mackey, Elizabeth Hansell, Patricia Doyle, Jiri Gut, Conor R. Caffrey, Julia Lehrman, Philip J. Rosenthal, James H. McKerrow, and Kelly Chibale. Synthesis and Structure – Activity Relationships of Parasiticidal Thiosemicarbazone Cysteine Protease Inhibitors against *Plasmodium falciparum, Trypanosoma brucei, and Trympanosoma cruzi.* J. Med. Chem. 2004, 47, 3212-3219.

[56] G.D. Kishore Kumar, Gustavo E. Chavarria, Amanda K. Charlton-Sevcik, Grace Kim Yoo, Jiangli Song, Tracy E. Strecker, Bronwyn G. Siim, David J. Chaplin, Mary Lynn Trawick, Kevin G. Pinney. Functionalized benzophenone, thiophene, pyridine, and fluorine thiosemicarbazone derivatives as inhibitors of cathepsin L. Bioorganic & Medicinal Chemistry Letters 20 (2010) 6610-6615.

[57] G.D. Kishore Kumar, Gustavo Chavarria, Amanda K. Charlton-Sevcik, Wara M. Arispe, Matthew T. MacDonough, Tracey E. Strecker, Shen-En Chen, Bronwyn G. Siim, David J. Chaplin, Mary Lynn Trawick, and Kevin G. Pinney. Design,

synthesis, and biological evaluation of potent thiosemicarbazone based cathepsin L inhibitors. Bioorganic & Medicinal Chemsitry Letters 20 (2010), 1415-1419.

[58] Melinda Soeung. Honors Thesis 2011.

[59] Robert A. Copeland. Evaluation fo Enzyme Inhibitors in Drug Discovery: A Guide for Medicinal Chemists and Pharmacologists. 2005. John Wiley & Sons, inc.

[60] Rick L. Tarleton, Richard Reithinger, Julio A. Urbina, Uriel Kitron, Ricardo E. Gurtler. The Challenges of Chaga' Disease – Grim Outlook of Glimmer of Hope? Plos Medicine. (2007) volume 4, issue 12.

[61] Louis V. Kirchhoff. American Trypanosomiasis (Chagas' Disease) – A Tropical Disease Now in the United States. The New England Journal of Medicine. 329: 639-644. (1993) no.9.

[62] Jose Milei, Roberto Andres Guerri-Guttenberg, Daniel Rodolfo Grana, and Ruben Storino. Prognostic impact of Chagas' disease in the United States.

[63] Caryn Bern, Sonia Kjos, Michael J. Yabsley, and Susan P. Montgomery. Clinical Microbiology Reviews, 2011, 655-681.

[64] Centers for Disease Control and prevention. Chagas' disease. http://www.cdc.gov/parasites/chagas/

[65] Jose Milei, Roberto Andres Guerri-Guttenberg, Daniel Rodolfo Grana and Ruben Storino. 2009. Prognostic impact of Chagas disease in the United States. *American Heart Journal,* 157, 22-29.

[66] Centers for Disease Control and Prevention. Parasites - American Trypanosomiasis (also known as Chagas Disease) http://www.cdc.gov/parasites/chagas/gen_info/vectors/index.html

[67] K.M. Tyler and D.M. Engman. The life cycle of *Trypanosoma cruzi* revisited. International Journal for Parasitology 31 (2001), 472-481.

[68] Alane Beatriz Vermelho et al. *Trypanasoma cruzi* Peptidases: An Overview. The Open Parasitology Journal, 2010, 4, 120-131.

[69] Anis Rassi Jr., Anis Rassi, Jose Antonio Martin-Neto. Chagas' Disease. Lancet, 2010, 375: 1388-1402.

[70] A.L Bodley and T.A. Shapiro. Molecular and cytotoxic effects of camptothecin, a topoisomerase I inhibitor on trypanosomes and Leishmanaia. PNAS 1995. 92:3726-3730.

[71] Guy F. Riou, Michtle Gabillot, Setha Douc-Rasy, Alain Kayser, Michel Barrois. A Type I DNA Topoisomerase from *Trypanosoma cruzi.* Eur. J. Biochem. 1983. 134, 479-484.

[72] Julio A. Urbino, Renee Lira, Gonzalo Visbal, Javier Bartroli. *In Vitro* antiproliferateive effects and mechanism of action of the new trixole derivative UR-9825 against protozoan parasite *Trypanosoma (Schizotrypanum) cruzi.* Antimicrobial Agent and Chemotherapy, 200, 2498-2502.

[73] Frederick S. Buckner, John H. Griffin, Aaron J. Wilson, Wesley C. Van Voorhis. Potent Anti-*trypanosoma cruzi* activiites of oxidosqualene cyclase inhibitors. Antimicrobial Agents and Chemotherapy, 2001, 1210-1215.

[74] Xiaohui Du, Chun Guo, Elizabeth Hansell, Patricia S. Doyle, Conor R. Caffrey, Tod P. Holler, James H. McKerrow, and Fred E. Cohen. Sythesis and Structure-Activity Relationship Study of a Potent Trypanocidal Thio Semicarbazone Inhibitor sof the Trypanosomal Cystein Protease Cruzain. J. Med. Chem 2002, 45, 2695-2707.

[75] Wagner A.S. Judice, Maria Helena S. Cezari, Ana Paula C.A. Lima, Julio Scharfstein, Jair Ribeiro Chagas, Ivarne L.S. Tersariol, Maria A. Juliano, and Luiz Juliano. Comparison of the specificity, stability, and individual rate constants with respective activation parameters for the peptidase activity of cruzipain and its recombinant form, cruzain, from *Trypanosoma cruzi.* Eur. J. Biochem. 268, 6578-6586 (2001)

[76] Cruzipain. http://www.uniprot.org/uniprot/P25779

[77] L. Huang, L.S. Brinen, and J.A. Ellman. Crystal structure of reversible ketone-based inhibitors of the cysteine protease cruzain. Bioorg. Med. Chem. (2003) 11: 21-29.

[78] Rogelio Siles, Shen-En Chen, Ming Zhou, Kevin G. Pinney, and Mary Lynn Trawick. Design, synthesis, and biochemical evaluation of novel cruzain inhibitors with potential application in the treatment of Chagas' disease. Bioorganic & Medicinal Chemistry Letters 16 (2006) 4405-4409.